

## Surf zone entrainment, along-shore transport, and human health implications of pollution from tidal outlets

S. B. Grant,<sup>1</sup> J. H. Kim,<sup>2</sup> B. H. Jones,<sup>3</sup> S. A. Jenkins,<sup>4</sup> J. Wasyl,<sup>4</sup> and C. Cudaback<sup>5</sup>

Received 29 March 2004; revised 14 June 2005; accepted 27 July 2005; published 22 October 2005.

[1] Field experiments and modeling studies were carried out to characterize the surf zone entrainment and along-shore transport of pollution from two tidal outlets that drain into Huntington Beach and Newport Beach, popular public beaches in southern California. The surf zone entrainment and near-shore transport of pollutants from these tidal outlets appears to be controlled by prevailing wave conditions and coastal currents, and fine-scale features of the flow field around the outlets. An analysis of data from dye experiments and fecal indicator bacteria monitoring studies reveals that the along-shore flux of surf zone water is at least 50 to 300 times larger than the cross-shore flux of surf zone water. As a result, pollutants entrained in the surf zone hug the shore, where they travel significant distances parallel to the beach before diluting to extinction. Under the assumption that all surf zone pollution at Huntington Beach originates from two tidal outlets, the Santa Ana River and Talbert Marsh outlets, models of mass and momentum transport in the surf zone approximately capture the observed tidal phasing and magnitude of certain fecal indicator bacteria groups (total coliform) but not others (*Escherichia coli* and enterococci), implying the existence of multiple sources of, and/or multiple transport pathways for, fecal pollution at this site. The intersection of human recreation and near-shore pollution pathways implies that, from a human health perspective, special care should be taken to reduce the discharge of harmful pollutants from land-side sources of surface water runoff, such as tidal outlets and storm drains.

**Citation:** Grant, S. B., J. H. Kim, B. H. Jones, S. A. Jenkins, J. Wasyl, and C. Cudaback (2005), Surf zone entrainment, along-shore transport, and human health implications of pollution from tidal outlets, *J. Geophys. Res.*, 110, C10025, doi:10.1029/2004JC002401.

### 1. Introduction

[2] Oceans adjacent to large urban communities, or “urban oceans,” are the final repositories of human waste from a myriad of sources [Culliton, 1998]. Historically, pollutant loading to the urban ocean was dominated by point sources of untreated or partially treated sewage [e.g., Murray et al., 2002]. Improvements in sewage treatment and disposal technology, together with better source controls, have progressed to the point that, nowadays, pollutant loading rates to the urban ocean are often dominated by non-point sources of pollution, typically in the form of dry and wet weather surface water runoff [Schiff et al., 2000]. Unlike sewage, which is typically discharged far offshore

through long submarine outfalls [Koh and Brooks, 1975], runoff flows into the ocean at the surfline where dilution is minimal and the likelihood of human contact is greatest [Inman and Brush, 1973]. In southern California, contamination of the surf zone by dry weather runoff apparently increases the risk that marine recreational bathers will contract diarrhea and other acute illnesses [Haile et al., 1999; Dwight et al., 2004]. In turn, illnesses caused by recreating in contaminated ocean waters have annual economic impacts ranging into the millions of dollars locally [Dwight et al., 2005] and into the billions of dollars globally [Shoval, 2003]. Dry and wet weather runoff from urban areas contains both human viruses [Jiang and Chu, 2004; Ahn et al., 2005; Jiang et al., 2001; C. Surbeck et al., Transport of suspended particles and fecal pollution in storm water runoff from an urban watershed in southern California, submitted to *Environmental Science and Technology*, 2005] and elevated concentrations of fecal indicator bacteria, the organisms tested for in most marine bathing water quality monitoring programs [Reeves et al., 2004]. Consequently, surface water runoff is a leading cause of beach health advisories and beach closures [Boehm et al., 2002a; Dwight et al., 2002; Kim and Grant, 2004; Kim et al., 2004].

[3] The focus of this paper is the dry weather contamination of shoreline bathing waters with fecal indicator

<sup>1</sup>Department of Chemical Engineering and Material Sciences, University of California, Irvine, California, USA.

<sup>2</sup>Department of Environmental Science and Engineering, Gwangju Institute of Science and Technology, Buk-gu, Gwangju, Korea.

<sup>3</sup>Department of Biological Sciences, University of Southern California, Los Angeles, California, USA.

<sup>4</sup>Scripps Institution of Oceanography, University of California, San Diego, California, USA.

<sup>5</sup>Marine Earth and Atmospheric Science, North Carolina State University, Raleigh, North Carolina, USA.

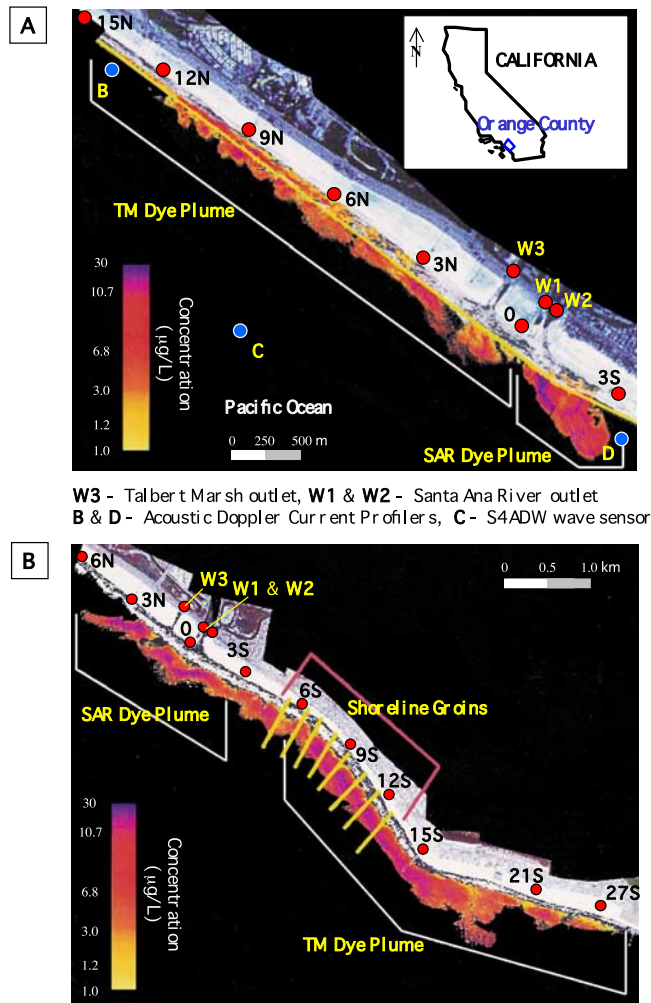


**Figure 1.** Areal images of dye released at the Santa Ana River (SAR) and the Talbert marsh (TM) outlets on (a) 1 May and (b) 10 May 2000. The blue circles denote the locations of current and wave sensors. The red circles denote the locations of sampling stations where fecal indicator bacteria concentrations were measured in the surf zone, and in the TM and SAR outlets, during the July 2001 experiment (described in section 3.2.2). Dye concentrations were measured in the surf zone at surf zone station 9N during the 1 May dye release (described in section 3.2.1.2).

bacteria from tidal outlets. At many coastal sites throughout the world, tidal outlets serve as the primary conduit through which mass is exchanged between the ocean and inland bodies of brackish water such as estuaries, salt water marshes, and marinas [Boer *et al.*, 2000; Elwany *et al.*, 1998; Kjerfve and Magill, 1989; Healy and Hickey, 2002]. When an inland body of water is contaminated by non-point sources of pollution (e.g., tainted surface water runoff, vessel waste discharges [Jeong *et al.*, 2005], its tidal outlet becomes a point source of shoreline pollution.

[4] The field and modeling studies reported in this paper focus on defining the impact of ebb flow from two tidal outlets—the Santa Ana River (SAR) and Talbert Marsh (TM) outlets—on water quality in the surf zone at Hunting-

ton Beach and Newport Beach in southern California during several dry weather periods in the summers of 2000 and 2001 (Figure 1). Consistent with marine bathing water standards in California and throughout the world [Bartram and Rees, 2000], in this study water quality is defined by the surf zone concentration of three groups of fecal indicator bacteria: total coliform (TC), *Escherichia coli* (EC), and enterococci bacteria (ENT). Four complementary studies are reported here: 1. Dye studies of the near-shore transport and mixing of tidal effluent from the SAR and TM outlets. 2. Hourly measurements of TC, EC, and ENT in tidal effluent from the SAR and TM outlets, and simultaneously at 10 stations in the neighboring surf zone. 3. Mass balance modeling of fecal indicator bacteria transport and reaction in the surf zone. 4. Momentum balance studies of wave-driven along-shore currents in the surf zone at Huntington Beach.

## 2. Field Site

[5] Huntington Beach and Newport Beach host over 5 million visitors per year, and both beaches have suffered chronic water quality problems in recent years. A risk modeling study concluded that the combination of a large number of visitors and chronically elevated fecal indicator bacteria concentrations in the surf zone at these two beaches could trigger tens of thousands of cases of diarrhea and other acute gastrointestinal diseases every year [Turbow *et al.*, 2003].

[6] The field data and modeling studies described in this paper focus in and around two tidal outlets—the SAR and TM outlets—that have been implicated as potential sources of fecal indicator bacteria in the surf zone at Huntington Beach and Newport Beach [Boehm *et al.*, 2002a; Grant *et al.*, 2001; Kim *et al.*, 2004]. The TM outlet exchanges water between a small (0.1 km<sup>2</sup>) tidal saltwater marsh and the ocean. The marsh, in turn, receives dry weather and storm runoff from a 55 km<sup>2</sup> region of the Talbert watershed located in the County of Orange. The SAR outlet drains several moderate-sized tidal salt water marshes (ca., 0.5 km<sup>2</sup>) and the SAR watershed, which encompasses 6,900 km<sup>2</sup> in the Counties of Orange, San Bernadino, and Riverside. As with many rivers in southern California, the SAR is not a river in the conventional sense, in that it has been highly modified to minimize flooding (i.e., significant stretches of the river are channelized and lined with concrete), there is little-to-no freshwater flow upstream of the tidal prism during dry weather periods, and any freshwater added to the tidal prism during dry weather periods typically derives from local sources of nuisance runoff—from the over-irrigation of lawns, car washing, etc.—which is often contaminated with very high concentrations of fecal indicator bacteria [Reeves *et al.*, 2004; Burton *et al.*, 1998].

[7] During dry weather conditions, flow through the TM and SAR outlets is tidally forced. Specifically, ocean water flows inland during flood tides, mixes with urban runoff from the surrounding community and non-point source pollution from within the tidal prism (e.g., sea gull feces deposited on the marsh mudflats [Grant *et al.*, 2000, 2001]), and contaminated water flows back through the tidal outlets and into the ocean during ebb tides. Water reclamation

activities upstream of the tidal prism capture virtually all flow in the SAR during dry weather periods, and hence all low-salinity water flowing into the tidal prisms in the SAR and TM outlets is from local sources of nuisance runoff, as noted earlier. The situation changes markedly during storms, when substantial volumes of storm water runoff from the Santa Ana River watershed can flow into the ocean from the SAR outlet, contributing fecal indicator bacteria, human pathogenic and bacterial viruses, and suspended particles to the surf zone and offshore [Ahn *et al.*, 2005].

[8] A detailed description of the Huntington Beach field site—including temporal and spatial patterns of fecal contamination in the surf zone, possible sources of this pollution, and the dynamics of tidal flow in the channels that drain to Huntington Beach—can be found elsewhere [Grant *et al.*, 2001; Boehm *et al.*, 2002a, 2002b, 2004a, 2004b; Sanders *et al.*, 2001; Kim *et al.*, 2004; Reeves *et al.*, 2004; Kim and Grant, 2004; Noble and Xu, 2004; L. Rosenfeld *et al.*, Temporal and spatial variability of fecal indicator bacteria in the surf zone off Huntington Beach, CA, submitted to *Marine Environmental Research*, 2005 (hereinafter referred to as Rosenfeld *et al.*, submitted manuscript, 2005)]. Studies of the generation and near-shore transport of storm water runoff plumes from river outlets in southern California, including the SAR, can also be found in the literature [Washburn *et al.*, 2003; Jones *et al.*, 2002; Warrick *et al.*, 2004; Ahn *et al.*, 2005].

### 3. Field Studies

#### 3.1. Materials and Methods

##### 3.1.1. Dye Studies

[9] Dye experiments were conducted during two dry weather periods in May 2000 to characterize the entrainment and along-shore transport of contaminants from the TM and SAR outlets. Rhodamine WT dye (Keystone, Santa Fe Springs, CA) was injected into the outlets of the TM and the SAR during two separate ebb tides, one on 1 May and another on 10 May 2000. The study on 1 May coincided with a spring tide when the tidal range was large (2.0 m); the study on 10 May coincided with a neap tide when the tide range was small (1.2 m). Rhodamine WT was chosen because it is relatively non-adsorbing and stable in ambient light [Smart and Laidlaw, 1977]. During the first experiment on 1 May, separate injections were carried out first in the TM outlet (1125–1155 PDT) and then in the SAR outlet (1245–1315 PDT). 20% (w/v) Rhodamine WT dye was pumped at a rate of  $4.2 \times 10^{-5} \text{ m}^3/\text{s}$  for approximately 30 minutes through a 5-meter PVC diffuser suspended in the middle of the channel. The evolution of the dye fields was followed over time using: 1. An airborne Digital Multi-Spectral Video sensor (DMSV Mk1 system, SpecTerra Systems, Nedlands, Australia) flown at approximately 1500 m. 2. Measurements of dye concentration in grab samples collected at stations 3N (N33°38.02' W117°58.03') and 9N (N33°38.57' W117°58.92'). The locations of the SAR and TM outlets, relative to surf zone stations 3N and 9N, are indicated in Figure 1. The concentration of Rhodamine WT in the grab samples was measured with a Turner Designs 10–005 fluorometer (Turner Designs, Inc, Sunnyvale, CA) that was calibrated with the Rhodamine WT stock that was used in the experiment. The fluorometer was

equipped with the Rhodamine WT filter set with excitation at 546 nm and emission at 570 nm. The injection protocol was repeated nine days later on 10 May 2000 when dye was released from the TM outlet (0810–0840 PDT) and the SAR outlet (0915–0945 PDT) during a single ebb tide.

##### 3.1.2. Fecal Indicator Bacteria Studies

[10] Water samples were collected hourly for 48 hours during a dry weather period from noon on 5 July to noon on 7 July (2001) by two different research teams—one from the University of California at Irvine (UCI) and another from the Orange County Sanitation District (OCS D)—at the following locations: 1. The UCI team collected water samples from the TM outlet, approximately 200 m upstream of where water from the marsh flows over the beach and into the ocean (station W3, Figure 1). 2. The UCI team collected water samples from two stations in the SAR outlet approximately 200 m upstream of where water from the river flows over the beach and into the ocean (stations W1 and W2, Figure 1). 3. The OCS D team collected water samples at ten surf zone stations located up-coast (north-west) and down-coast (south-east) of the SAR and TM outlets (stations 15S, 9S, 3S, 0, 3N, 6N, 9N, 12N, 15N, 21N, Figure 1; note station 21N is off of the map). The surf zone stations are designated by OCS D according to their distance (in feet) north or south of the SAR outlet; e.g., stations 6N and 9S are located 6000 feet up-coast and 9000 feet down-coast of the SAR outlet. To characterize spatial variability in the concentration of fecal indicator bacteria across the SAR outlet (i.e., transverse to the direction of tidal flow), the UCI team collected separate samples from the top and bottom of the water column at the up-coast (station W1) and down-coast (station W2) sides of the river outlet (i.e., four samples were collected from the cross-section of the SAR outlet every hour). Details of the TM and SAR outlet sampling can be found in Grant *et al.* [2002]; details of the surf zone sampling can be found in Noble and Xu [2004]. In brief, water samples were immediately placed on ice, and transported to OCS D (surf zone samples) or UCI (SAR and TM outlet samples) where they were analyzed for TC, EC and ENT using defined substrate tests known commercially as Colilert and Enterolert, implemented in a 96 well quantitray format (IDEXX, Westbrook, MN).

### 3.2. Results

#### 3.2.1. Dye Experiments

##### 3.2.1.1. Areal Observations of Dye Fields

[11] Environmental conditions during the four dye experiments, together with inferred along-shore mixing parameters (described below), are summarized in Table 1. Areal images of the dye fields reveal three distinct near-shore transport processes (Figure 1). Process 1: As dye-labeled water from the tidal outlets flowed over the beach and into the ocean during ebb tides, a portion was carried directly offshore in a momentum jet formed by ebb flow from the outlet, and the rest was entrained in the surf zone. Process 2: The portion of dye-labeled water entrained in the surf zone was transported parallel to the shore by wave-driven surf zone currents (referred to below as along-shore advection) and transported seaward by cross-shore currents (e.g., rip and undertow currents). Process 3: The portion of dye-labeled water taken seaward by cross-shore currents dis-

**Table 1.** Environmental Conditions During the Dye Experiments and Comparison of Predicted and Observed Along-Shore Plume Stretching

| Date        | Time, PDT         | Elapsed Time After the End of Dye Release, s | Wave Height by S4 Wave Sensor, m | Wave Direction <sup>a</sup> by S4 Wave Sensor (Azimuth) | Observed TM Dye Plume Length by DMSV Pixels, m | $D_{eff}$ , m/s | Predicted TM Dye Plume Length by $L \approx 4\sqrt{2D_{eff}t}$ , m |
|-------------|-------------------|----------------------------------------------|----------------------------------|---------------------------------------------------------|------------------------------------------------|-----------------|--------------------------------------------------------------------|
| May 1 2000  | 11:55             | 0                                            | 0.75                             | S (180°)                                                | $3.6 \times 10^2$ <sup>b</sup>                 |                 |                                                                    |
|             | 14:30 (Figure 1a) | $9.3 \times 10^3$                            | 0.65                             | S (180°)                                                | $3.6 \times 10^3$                              | 40              | $3.5 \times 10^3$                                                  |
|             | 17:33             | $2.0 \times 10^4$                            | 0.95                             | S (180°)                                                | $5.3 \times 10^3$                              |                 | $5.1 \times 10^3$                                                  |
| May 10 2000 | 08:40             | 0                                            | 1.4                              | S (200°)                                                | $1.8 \times 10^2$ <sup>b</sup>                 |                 |                                                                    |
|             | 15:18 (Figure 1b) | $2.4 \times 10^4$                            | 1.3                              | W (270°)                                                | $7.9 \times 10^3$                              | 80              | $7.8 \times 10^3$                                                  |
|             | 16:05             | $2.7 \times 10^4$                            | 1.3                              | W (270°)                                                | $8.3 \times 10^3$                              |                 | $8.3 \times 10^3$                                                  |

<sup>a</sup>Waves are out of the south (S) when wave directions are less than 216°, and waves are out of the west (W) when wave directions are greater than 216°.

<sup>b</sup>Values were estimated by  $F_l \Delta t_{dye}$  where  $F_l$  and  $\Delta t_{dye}$  represent the long-shore velocity (= 0.3 m/s) during the dye-release and the duration of dye-release, respectively.

persed offshore and a fraction recycled back into the surf zone.

[12] All three processes are evident in Figure 1a, where the spatial distribution of dye-labeled water is visualized at 14:30 PDT on 1 May, approximately 2.5 h after the conclusion of the TM dye injection and 1.25 hours after the end of the SAR dye injection. A portion of the dye-labeled water from the TM outlet jetted directly offshore of the outlet (Process 1), and the rest was entrained in the surf zone where it advected parallel to the beach at approximately 0.3 m/s (Process 2, labeled “TM Dye Plume” in Figure 1a). The yellow curve drawn parallel to the shore in Figure 1a roughly demarcates the boundary between the surf zone and offshore. In this case, the along-shore current in the surf zone was directed up-coast because ocean waves with average significant heights of 0.7 to 1 m were from the south (see Table 1), as is frequently the case for this area of southern California during the summer. The series of small dye plumes seaward of the surf zone (i.e., seaward of the yellow line in Figure 1a) between 6N and 12N reflect the cross-shore transport of dye-labeled surf zone water by rip currents. Once seaward of the surf zone, this dye-labeled water gradually dispersed offshore, and a fraction recycled back into the surf zone as will be documented below (Process 3).

[13] A significant fraction of the dye-labeled water released from the SAR outlet on 1 May was ejected seaward of the surf zone in the momentum jet formed by ebb flow from the SAR outlet (labeled “SAR Dye Plume” in Figure 1a). Once seaward of the surf zone, this dye field slowly drifted offshore and down coast, consistent with acoustic Doppler current profiler (ADCP) data collected at stations B and D (blue dots in Figure 1a) which indicate that along-shore currents just seaward of the surf zone were weakly down-coast (<0.10 m/s, data not shown). Two hours following the image in Figure 1a, dye-labeled water in the surf zone continued to transport up-coast at about 0.2 m/s while, seaward of the surf zone, dye-labeled water advected very slightly up-coast as the currents outside the surf zone changed direction in response to the shift from an ebb to a flood tide.

[14] A second set of dye injections were performed on 10 May when waves were out of the west (significant height of 1.3 to 1.4 m, see Table 1). The dye injection protocol on 10 May was similar to that used on 1 May: dye was first injected in the TM outlet, and then in the SAR outlet

approximately 1 h later. Most dye-labeled water from the TM outlet entrained in the surf zone where it advected down-coast at slightly less than 0.3 m/s, and transported seaward of the surf zone by rip currents (labeled “TM Dye Plume” in Figure 1b). A series of groins down-coast of the SAR outlet—represented by a series of yellow lines along the beach in Figure 1b (note that these lines do not represent the physical dimension of groins)—caused perturbations in the dye field. Immediately down-coast of the eastward bend in the coastline, a portion of the dye-labeled water from the TM outlet separated from the coast producing a small offshore plume. A significant fraction of the dye field from the SAR outlet was transported seaward of the surf zone by the momentum jet formed by ebb flow from the SAR (labeled “SAR Dye Plume” in Figure 1b). Once offshore of the surf zone, the dye-labeled water transported slightly up-coast until late afternoon when the along-shore current seaward of the surf zone changed direction to down-coast in phase with the change from a flood to an ebb tide.

[15] Based on the results from the two dye experiments (on 1 and 10 May) the following transport patterns can be identified. In both field experiments, a large fraction of the SAR effluent was carried seaward of the surf zone by a momentum jet, where it was transported by coastal currents, the along-shore component of which changes direction with the phase of the tide (predominantly up-coast during flood tides, and down-coast during ebb tides [Kim *et al.*, 2004]). A large fraction of the TM effluent, on the other hand, entrained in the surf zone where it was advected up-coast or down-coast (at ca. 0.3 m/s) depending on the direction of the approaching wave field (up-coast during south to south-west swells, down-coast during west swells) and seaward by cross-shore currents (rip currents and undertows).

[16] Given the very limited number of realizations reported here ( $n = 2$  for each outlet), it would be imprudent to suggest that these are the only transport patterns that operate at our field site. Rather, the remarkably divergent entrainment and transport patterns reported here for the TM and SAR dye fields—which were released about 1 hour apart and initially separated in space by no more than 300 m—underscores the degree to which the near-shore fate and transport of effluent from the TM and SAR outlets is influenced by multiple and potentially interacting factors, including the momentum associated with ebb flow from the TM and SAR outlet, prevailing wave fields and coastal

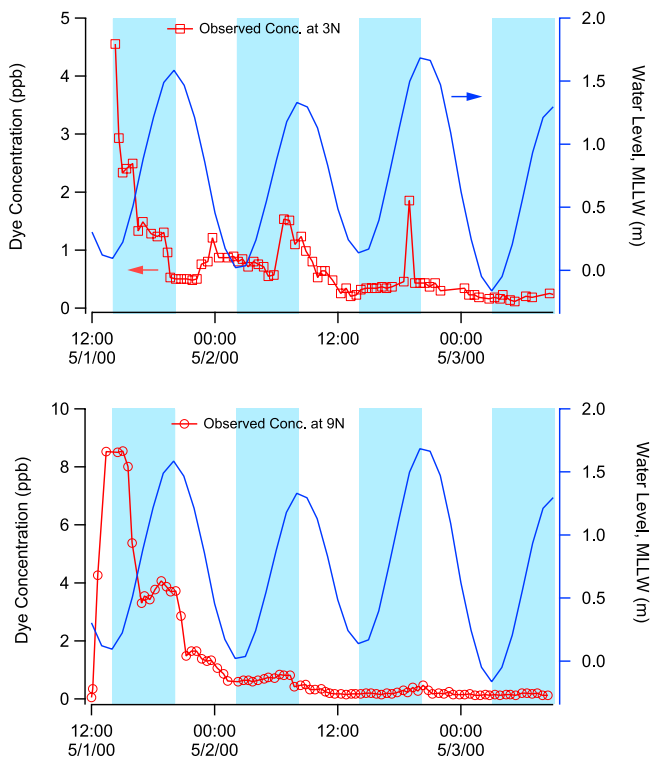


**Figure 2.** Dye concentration (red lines and markers) measured in the surf zone at (top) 3N and (bottom) 9N. Blue curves indicate the measured Mean Lower Low Water (MLLW) level. Vertical blue stripes indicate periods of rising tide.

currents, and fine-scale features of the flow field around the two outlets.

### 3.2.1.2. In Situ Observations of Dye Fields

[17] Figure 2 presents measurements of dye concentration in the surf zone at stations 3N (top panel) and 9N (bottom panel) during and following the TM and SAR dye injections on 1 May 2000. The following temporal patterns are evident at both stations: 1. A single large dye pulse appears early in the time series (referred to here as the “primary pulse”). 2. A sequence of smaller pulses, many of which coincide with flood tides, appear later in the time series (referred to here as “secondary pulses”). Sampling at surf zone station 3N did not commence early enough to capture the leading edge of the primary pulse, but the trailing edge of the primary pulse is well defined at this station (top panel in Figure 2). The leading and trailing edges of the primary pulse are well defined at 9N; however, dye measurements saturated at a concentration of 8.5 ppb and hence the peak concentration of the primary pulse at 9N is not known.

[18] In the last section we noted that most of the dye-labeled water from the SAR outlet was ejected offshore in a momentum jet on 1 May. Hence, the primary dye pulse detected at 3N and 9N probably corresponds to the up-coast advection of dye-labeled water originating from the TM outlet. This conclusion is supported by the arrival time of the primary pulse at 9N. Under the assumption that the primary pulse originated from the TM dye injection, the arrival time of the primary pulse at 9N implies an up-coast transport velocity of 0.3 m/s, which is equal to the along-

shore transport velocity of dye-labeled surf zone water independently estimated from the areal images (see last section).

[19] In considering the origin of the secondary pulses, it is important to keep in mind that dye measurements were carried out on water samples collected from ankle depth in the surf zone; in other words, the sampling points at 3N and 9N migrated up and down the beach face with the rise and fall of the tides. With this point in mind, at least two hypotheses can be formulated to explain the origin of the secondary pulses. Hypothesis 1: it takes several flood/ebb cycles to completely flush out to the ocean dye injected into the TM and SAR outlets, and hence the secondary pulses reflect the up-coast transport of dye-labeled water from the TM and/or SAR outlets released over multiple consecutive ebb tides. Hypothesis 2: the secondary pulses arise from the recycling back into the surf zone of dye that was initially ejected seaward by rip currents and/or outlet momentum jets.

[20] Multiple lines of evidence favor the second, over the first, hypothesis. First, assuming an along-shore transport velocity of 0.3 m/s it would take  $<1$  h for effluent ejected from the TM and SAR outlets during ebb tides to reach surf zone station 3N. However, a comparison of the blue and red curves in Figure 2 (top panel) reveal that all but one of the secondary pulses at 3N peak during flood tides, between 3 to 5 h after the end of the ebb tide. Second, dye-labeled water is not evident on the areal images (Figure 1a) in the inland portions of the SAR and TM outlets during and shortly after the dye injection event. These two observations—that the tidal phasing of the secondary pulses is inconsistent with their being released from the TM and/or SAR outlets over multiple ebb events, and that areal images fail to demonstrate significant concentrations of dye left in the TM and SAR outlets post initial release—appear to rule out Hypothesis 1.

[21] The second hypothesis is consistent with areal images of the dye field that show dye-labeled water lingering just seaward of the surf zone for at least 24 h after the dye was released on 1 May (data not shown). Presumably, dye-labeled water just offshore of the surf zone could mix back into the surf zone by rip-current driven circulation cells. Over this stretch of beach, the exchange of water between the surf zone and offshore is influenced by a thermal boil generated by the submarine discharge of waste heat from a local power plant seaward of surf zone station 9N [KOMEX  $H_2O$  Science Incorporated, 2003]. The observation that the secondary pulses occur during flood tides may result from the interaction between this thermal boil (which apparently enhances cross-shore transport) and the tidal component of the along-shore current just seaward of the surf zone (which transports water up-coast during flood tides and down-coast during ebb tides). The influence of the thermal boil on cross-shore transport at Huntington Beach will be described in detail elsewhere (B. H. Jones et al., manuscript in preparation, 2005).

### 3.2.1.3. Along-Shore and Cross-Shore Flux of Dye-Labeled Water

[22] In this section we present an analysis of the in situ dye measurements collected during the TM dye injection on 1 May, 2000 with the goal of obtaining a first-order estimate of the along-shore and cross-shore flux of water in the surf

**Table 2.** Description and Magnitude of Key Surf Zone Transport Variables

| Parameters           | Values                                         | Units                                          | Description                                                                                                                                                                                              |
|----------------------|------------------------------------------------|------------------------------------------------|----------------------------------------------------------------------------------------------------------------------------------------------------------------------------------------------------------|
| $\tau$               | 100 to 1000                                    | s                                              | timescale over which model parameters are averaged                                                                                                                                                       |
| $y$                  | -5000 to +7000 <sup>a</sup>                    | m                                              | along-shore distance from the mouth of the SAR outlet (positive $y$ points up-coast)                                                                                                                     |
| $y_{SAR}$            | 0                                              | m                                              | $y$ -coordinate of the Santa Ana River outlet                                                                                                                                                            |
| $y_{TM}$             | 300 <sup>a</sup>                               | m                                              | $y$ -coordinate of the Talbert Marsh outlet                                                                                                                                                              |
| $y_{9N}$             | 3000 <sup>a</sup>                              | m                                              | $y$ -coordinate of surf zone station 9N                                                                                                                                                                  |
| $\Delta y$           | —                                              | m                                              | some fixed along-shore distance                                                                                                                                                                          |
| $x_w$                | 50 <sup>a</sup>                                | m                                              | width of the well-mixed region of the surf zone                                                                                                                                                          |
| $h_w$                | 1.0 <sup>a</sup>                               | m                                              | water depth at the offshore edge of the well-mixed region of the surf zone                                                                                                                               |
| $A_c = x_w h_w / 2$  | 25 <sup>a</sup>                                | m <sup>2</sup>                                 | cross-shore area of the well-mixed region of the surf zone                                                                                                                                               |
| $A_l = h_w \Delta y$ | —                                              | m <sup>2</sup>                                 | along-shore area of the well-mixed region of the surf zone (magnitude depends on choice of $\Delta y$ )                                                                                                  |
| $v_l$                | NA <sup>d</sup>                                | ms <sup>-1</sup>                               | along-shore component of the local surf zone velocity                                                                                                                                                    |
| $v_c$                | NA <sup>d</sup>                                | ms <sup>-1</sup>                               | cross-shore component of the local surf zone velocity                                                                                                                                                    |
| $F_l$                | 0.3 <sup>a</sup>                               | ms <sup>-1</sup>                               | along-shore flux of surf zone water (see equation (1a))                                                                                                                                                  |
| $F_l A_c$            | 8 <sup>a</sup>                                 | m <sup>3</sup> s <sup>-1</sup>                 | along-shore flow rate of surf zone water                                                                                                                                                                 |
| $F_c$                | <10 <sup>-3</sup> to <10 <sup>-2a</sup>        | ms <sup>-1</sup>                               | cross-shore flux of surf zone water (see equation (1b))                                                                                                                                                  |
| $M(y)$               | 0 to 4 <sup>a</sup>                            | kg                                             | mass of pollutant or tracer passing a fixed location along the shore (at coordinate $y$ ) over an extended period of time                                                                                |
| $M_{dye}$            | 8.6 <sup>a</sup>                               | kg                                             | mass of dye injected into the Talbert Marsh during the 1 May 2000 dye experiment                                                                                                                         |
| $M_{9N}$             | >0.71 <sup>a</sup>                             | kg                                             | mass of dye that passed surf zone station 9N following the dye release from the Talbert marsh on 1 May 2000                                                                                              |
| $\alpha$             | 0 to 0.5 <sup>a</sup>                          | —                                              | fraction of pollutant or tracer mass flowing out of a tidal outlet that is entrained in the surf zone                                                                                                    |
| $\alpha_{i,j}$       | 0 to 0.5 <sup>a</sup>                          | —                                              | fraction of pollutant or tracer mass that is entrained in the surf zone from the $j$ th tidal outlet at the $i$ th time                                                                                  |
| $C_{i,j}$            | <10 <sup>1</sup> to >10 <sup>4.38a</sup>       | MPN/100 mL                                     | concentration of fecal indicator bacteria discharged to the surf zone from the $j$ th tidal outlet at the $i$ th time in units of most probable number (MPN) per 100 mL of sample                        |
| $Q_{i,j}$            | -100 to 100 <sup>a</sup>                       | m <sup>3</sup> s <sup>-1</sup>                 | Tidal volumetric flow rate into the surf zone from the $j$ th tidal outlet at the $i$ th time (negative values denote flood tides, positive values denote ebb tides)                                     |
| $M_{i,j}$            | 0 to 10 <sup>10a</sup>                         | MPN/s                                          | Tidal mass loading rate of fecal indicator bacteria into the surf zone from the $j$ th tidal outlet at the $i$ th time (note that during flood tides $M_{i,j}$ is set to zero, see equation (11a) (11b)) |
| $k_{eff}$            | 4 × 10 <sup>-5a</sup>                          | s <sup>-1</sup>                                | effective first-order decay constant, including effects of cross-shore dilution and die-off (see equation (6b))                                                                                          |
| $k_{FIB}$            | 2.7 × 10 <sup>-7</sup> to 5 × 10 <sup>-7</sup> | W <sup>-1</sup> m <sup>2</sup> s <sup>-1</sup> | solar-modulated first-order die-off rate (see constants below specific for the different fecal indicator bacteria groups)                                                                                |
| $I(t)$               | 0 to 1000 <sup>a</sup>                         | Wm <sup>-2</sup>                               | solar radiation                                                                                                                                                                                          |
| $k = k_{FIB} I(t)$   | 0 to 5 × 10 <sup>-4c</sup>                     | s <sup>-1</sup>                                | First-order die-off rate of fecal indicator bacteria                                                                                                                                                     |
| $k_{TC}$             | 5 × 10 <sup>-7c</sup>                          | W <sup>-1</sup> m <sup>2</sup> s <sup>-1</sup> | solar-modulated first-order die-off rate for total coliform                                                                                                                                              |
| $k_{FC}$             | 4.7 × 10 <sup>-7c</sup>                        | W <sup>-1</sup> m <sup>2</sup> s <sup>-1</sup> | solar-modulated first-order die-off rate for fecal coliform (taken here to be the same as for <i>Escherichia coli</i> , EC)                                                                              |
| $k_{ENT}$            | 2.7 × 10 <sup>-7c</sup>                        | W <sup>-1</sup> m <sup>2</sup> s <sup>-1</sup> | solar-modulated first-order die-off rate for enterococci                                                                                                                                                 |
| $D_L$                | 60–70 <sup>b</sup>                             | m <sup>2</sup> s <sup>-1</sup>                 | longitudinal dispersion coefficient for along-shore mixing                                                                                                                                               |
| $\varepsilon$        | NA <sup>d</sup>                                | m <sup>2</sup> s <sup>-1</sup>                 | turbulent diffusion coefficient for along-shore mixing                                                                                                                                                   |
| $D_{eff}$            | 40–80 <sup>a</sup>                             | m <sup>2</sup> s <sup>-1</sup>                 | effective diffusion constant for along-shore mixing (see equation (6a))                                                                                                                                  |
| $Pe$                 | 0 to 20 <sup>a</sup>                           | —                                              | Peclet number (see equation (14b) for definition)                                                                                                                                                        |
| $Br$                 | 0.1 <sup>a</sup>                               | —                                              | Brooks number (see equation (14c) for definition)                                                                                                                                                        |

<sup>a</sup>Estimated from field data reported in this study.

<sup>b</sup>Estimated by *Inman et al.* [1971].

<sup>c</sup>Estimated by *Sinton et al.* [1999].

<sup>d</sup>Not available.

zone. This analysis could be applied only to the TM dye injection on 1 May because, during the other dye injections, either very little dye entrained in the surf zone (injection at the SAR outlets) or the entrained dye did not pass the sampling locations at surf zone stations 3N and 9N (TM dye injection on 10 May).

[23] For the purposes of this analysis, we imagine a well-mixed region of the surf zone of length  $\Delta y$ , width  $x_w$ , and depth at the offshore edge of  $h_w$ . The cross-shore area of this mixed zone is therefore  $A_c = x_w h_w / 2$  (units L<sup>2</sup>) and the along-shore area is  $A_l = h_w \Delta y$ . The same parameterization is

employed later to develop an unsteady model of pollutant reaction and transport in the surf zone (section 4.1.2, see also Table 2). Fluxes of surf zone water in the along-shore and cross-shore directions (represented by  $F_l$  and  $F_c$ , units of L/T) are defined (in equations 1a and 1b) as the average of the along-shore and cross-shore components of the surf zone current (represented by  $v_l$  and  $v_c$ , units L/T).

$$F_l = \int_{A_c} v_l dA / A_c \quad (1a)$$

$$F_c = \int_{A_l} v_c dA / A_l \quad (1b)$$

[24] On May 1, 2000, 4.5 kg of dye was injected into the surf zone at the Talbert Marsh outlet (a total of 9 kg was injected into the TM outlet, and approximately 50% of that immediately entrained into the surf zone [Grant *et al.*, 2001]), and over the following two days some fraction of this dye was detected in the surf zone at several locations (i.e., 3N and 9N) up-coast of the TM outlet. We estimate the total mass of dye that passed beach station 9N by adding up the observed concentrations over time, thus:

$$M(y) = \sum F_l A_c C(y) \Delta t \quad (2)$$

[25] The sum in equation (2) is taken over all samples collected in the surf zone at 9N,  $C(y = 9N)$  represents a single observation of the dye concentration at 9N in  $\text{kg/m}^3$ ,  $F_l$  and  $A_c$  are defined above, and  $\Delta t$  is the time interval between sampling events ( $\Delta t = 1$  h). We assumed that along-shore flux  $F_l$  is equal to the observed shore-parallel propagation velocity of dye-labeled water in the surf zone, which was estimated in section 3.2.1.1 from aerial photos of the dye fields:  $F_l = 0.3$  m/s. The width of the surf zone,  $x_w = 50$  m, is also estimated from aerial photos, and the water depth,  $h_w = 1$  m, is estimated from measurements of the beach profile. The along-shore volume flow rate in the surf zone,  $F_l A_c$  is thus estimated to be  $8 \text{ m}^3/\text{s}$ . Substituting into equation (2) values for  $C(y = 9N)$ ,  $F_l$ ,  $x_w$ , and  $h_w$ , we obtain the following lower-bound for the mass of dye passing surf zone station 9N:  $M(y = 9N) > 0.7$  kg, a modest fraction of the original injection. Note that this estimate is a lower bound because dye measurements in the surf zone saturated as the primary dye pulse passed 9N (see lower panel of Figure 2).

[26] An estimate for the cross-shore flux  $F_c$  can be obtained by combining the lower-bound for  $M(y = 9N) > 0.7$  kg with a model of surf zone transport and mixing:

$$M(y) = M_0 \exp \left[ \frac{-2yF_c}{x_w F_l} \right] \quad (3)$$

where  $M(y)$  is the total mass of dye passing a surf zone station located a distance  $y$  down-current from the source,  $M_0$  represents the mass of dye entrained in the surf zone at  $y = 0$  (taken here as the outlet of the Talbert Marsh), and all other variables have been defined previously (also see Table 2). This simple model for the mass of pollutant (or tracer) passing a fixed point along the shoreline can be derived [see Boehm, 2003] under the assumption that mass transport in the surf zone is controlled by a steady-state balance between along-shore advection (represented by  $F_l$ ) and cross-shore dilution (represented by  $F_c$ ). As demonstrated in section 4.2.1 of this paper, equation (3) can also be derived using a more realistic unsteady model of surf zone fate and transport, provided that along-shore advection dominates both along-shore mixing (by longitudinal dispersion and/or turbulent diffusion) and pollutant loss from the surf zone (by cross-shore mixing and/or first-order reaction).

[27] Substituting into equation (3) values for  $y = 9N = 2.5$  km,  $F_l = 0.3$  m/s,  $x_w = 50$  m,  $M_0 = 4.5$  kg, and  $M(y = 9N) > 0.7$  kg, the following estimate for the cross-shore flux of surf zone water is obtained:  $F_c < 0.006$  m/s. According to this calculation, the flux of surf zone water parallel to shore is  $>50$  times larger than the flux of surf zone water cross-shore:  $F_l/F_c > 50$ . This result is qualitatively consistent with the aerial image in Figure 1a that shows dye from the TM outlet is highly elongated in the shore-parallel direction. An independent estimate of  $F_c$ , based on application of the above model to fecal indicator bacteria measurements in the surf zone, is reported later in the paper (section 3.2.2.2).

#### 3.2.1.4. Along-Shore Stretching of Dye Fields in the Surf Zone

[28] Based on the areal images in Figure 1, it is clear that dye labeled water in the surf zone undergoes significant stretching in the along-shore direction. Here we show that a Fickian diffusion model adequately describes this along-shore stretching and—at least for the set of experiments reported here—along-shore mixing appears to be dominated by longitudinal dispersion.

[29] If a Fickian diffusion model applies, then the along-shore length  $L$  of the dye field should increase with time thus [Fischer *et al.*, 1979]:

$$L \approx 4\sqrt{2D_{eff}t} \quad (4)$$

where  $t$  is elapsed time since the dye was injected and the effective diffusion coefficient  $D_{eff} = \varepsilon + D_L$  (units of  $\text{L}^2/\text{T}$ ) is taken as the sum of coefficients for turbulent diffusion  $\varepsilon$  and longitudinal dispersion  $D_L$ . The lengths of dye plumes in the surf zone at various times post release (Table 1) are consistent with the predicted relationship between  $L$  and  $t$  in equation (4). Referring to Table 1, the predicted and observed plume lengths are in near perfect agreement for the second time point (14:30 PDT on 1 May and 15:18 PDT on 10 May), because the magnitude of  $D_{eff}$  was calculated from this first set of observations. Significantly, the predicted and observed lengths for the third time point (17:33 PDT on 1 May and 16:05 PDT on 10 May) are also in close agreement. Our estimates of the along-shore mixing coefficient (40 to 80  $\text{m}^2/\text{s}$ , see Table 1) are comparable to the longitudinal dispersion coefficients of 60 to 70  $\text{m}^2/\text{s}$  inferred from rip current spacing and along-shore current measurements by Inman *et al.* [1971] at another southern California beach. This last observation is consistent with the idea that longitudinal dispersion dominates the along-shore stretching, and hence mixing, of mass in the surf zone.

#### 3.2.2. Fecal Indicator Bacteria Experiments

##### 3.2.2.1. Observations of Fecal Indicator Bacteria in the Outlets and Surf Zone

[30] Hourly measurements of fecal indicator bacteria in the surf zone and SAR and TM outlets are more-or-less consistent with the hypothesis that these tidal outlets are a source of fecal pollution in the surf zone. Fecal indicator bacteria measurements are presented in Figure 3, where the log-transformed concentrations of TC, EC, and ENT in the surf zone are denoted by color, with red roughly corresponding to California's single-sample ocean bathing water standards for the respective indicator bacteria and blue corresponding to the lower-limit of detection of the

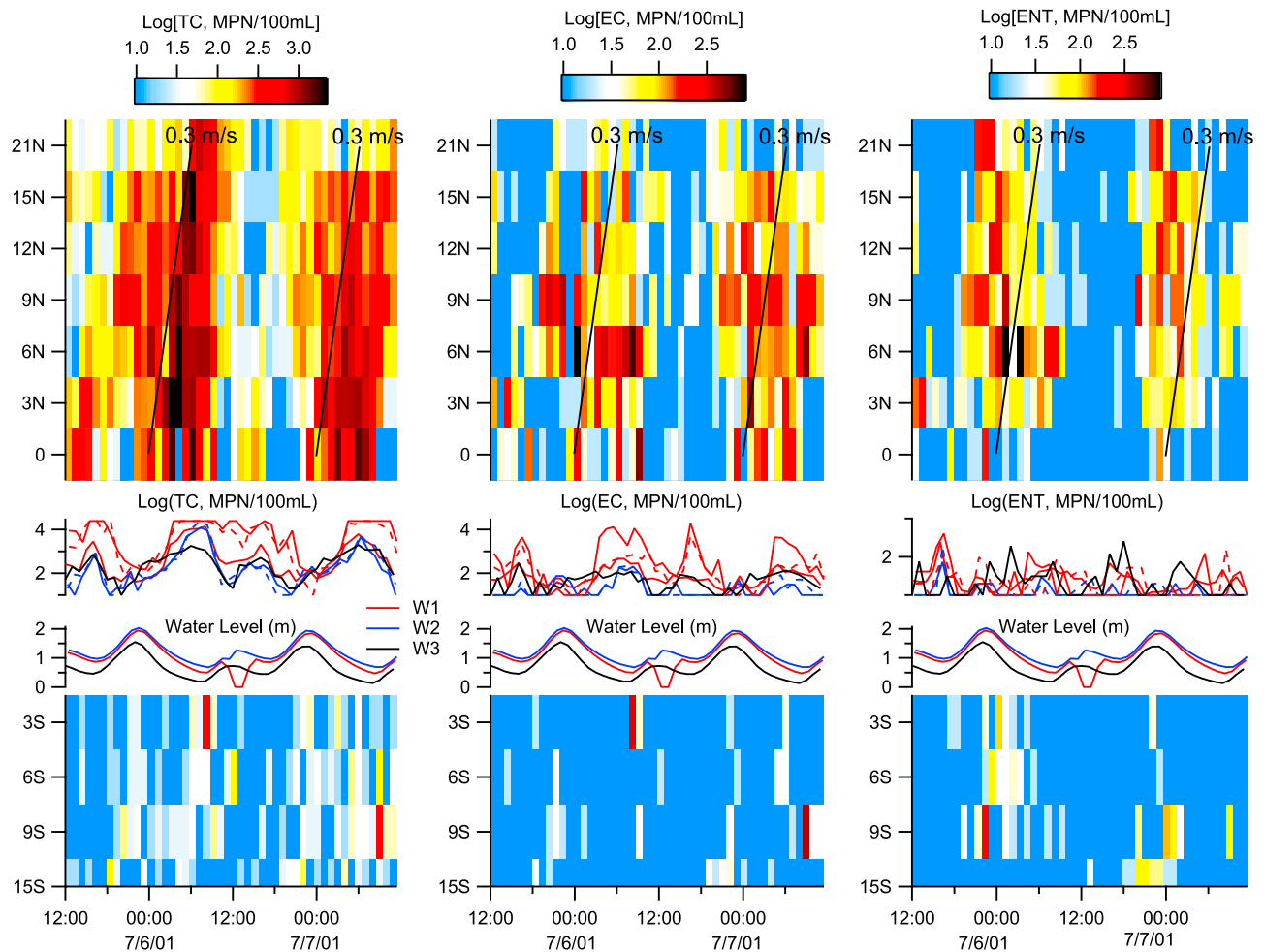


**Figure 3.** Hourly measurements of fecal indicator bacteria in the surf zone at Huntington Beach (surf zone stations 0 through 21N, top set of panels) and at Newport Beach (surf zone stations 3S through 15S, bottom set of panels) over a 48 h period, noon on 5 July to noon on 7 July (2001). Colors represent the log-transformed concentration of three different groups of fecal indicator bacteria: total coliform (TC), *Escherichia coli* (EC), and enterococci bacteria (ENT). Hourly measurements of water level and fecal indicator bacteria concentration in the Talbert and Santa Ana River outlets (stations W1, W2, and W3) are indicated by colored curves (red, blue, and black) in the center panels; solid and dashed curves represent surface and bottom water samples, respectively. A subset of the data presented in this figure, specifically, the surf zone data, are also included in the following publications: Kim *et al.* [2004], Noble and Xu [2004], and Rosenfeld *et al.* (submitted manuscript, 2005).

assays used in this study (10 MPN/100 mL). For the purposes of this paper, the units “MPN/100mL” can be interpreted as a measure of bacterial number or mass per volume of water sample. In general, the highest concentrations of fecal indicator bacteria were measured on the up-coast side of the SAR and TM outlets (i.e., stations 0 through 21N), and the lowest concentrations were measured on the down-coast side of these two outlets (i.e., stations 3S through 15S). Further, fecal contamination on the up-coast side of the SAR and TM outlets tends to occur in discrete ca. 6 h pulses that roughly coincide with the midnight ebb tide (compare red streaks in Figure 3 with water level measured in the SAR and TM outlets at stations W1, W2, and W3). During this field experiment, waves were out of the south to south-west, and hence wave-driven currents in the surf zone were probably directed up-coast (see section 4.2.3). Collectively, these three observations—1. The SAR

and TM outlets demarcate the down-coast edge of the worst surf zone contamination; 2. Pulses of contamination are roughly coincident with the large midnight ebb tide when water from the two outlets flows over the beach and into the ocean; 3. Breaking waves were out of the south to south-west and hence likely to generate up-coast directed currents in the surf zone—implicate tidal outflow from the SAR and TM outlets as a significant source of fecal indicator bacteria pollution in the surf zone at our field site.

[31] While the results presented in Figure 3 generally implicate tidal outflow from the SAR and TM outlets as a source of fecal indicator bacteria in the neighboring surf zone, the details of how this process occurs are complex and only partially illuminated by the present study. For example, hourly measurements of fecal indicator bacteria concentration across the SAR outlet reveal a remarkable degree of variability over the river mouth (i.e., transverse to the

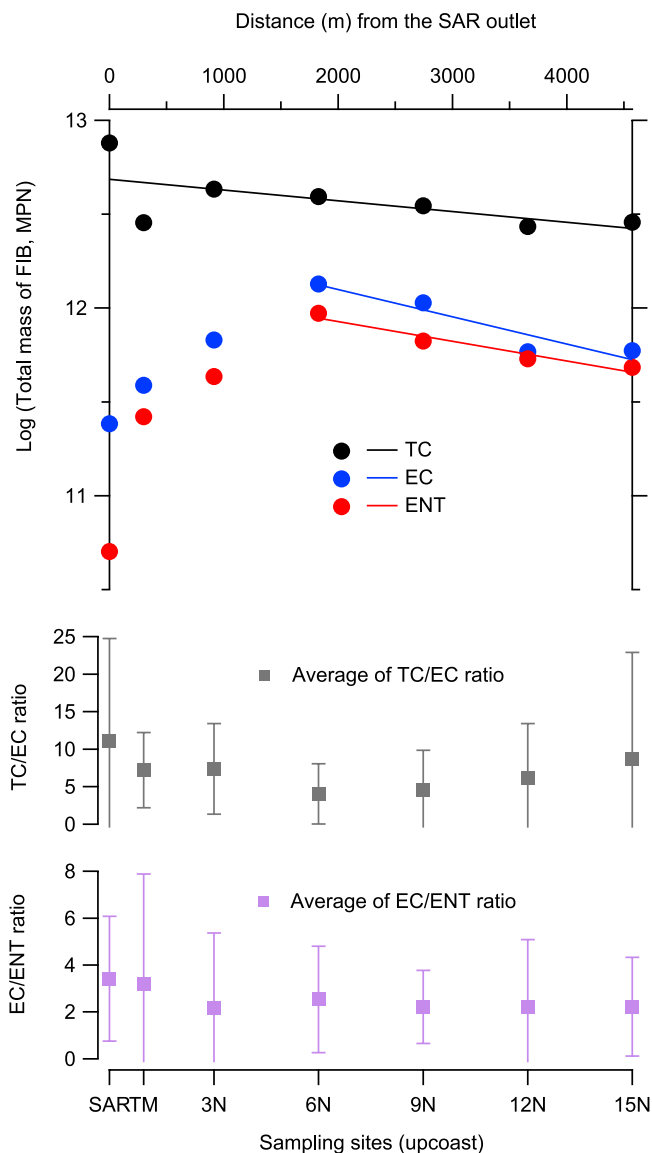


**Figure 4.** Total mass of fecal indicator bacteria that flowed out of the SAR and TM outlets, and flowed past the upcoast surf zone stations, during the 48-hour study on 5–7 July, 2001 at Huntington State Beach (top panel). Also shown are the average (and standard deviation) of two fecal indicator bacteria ratios: TC/EC (middle panel) and EC/ENT (bottom panel).

direction of tidal flow), with concentrations frequently >100 times higher on the down-coast side of the river outlet compared to the up-coast side (compare fecal indicator bacteria concentrations measured at stations W1 and W2, red and blue curves, middle panel, Figure 3). As described elsewhere [Grant *et al.*, 2002], water quality on the down-coast edge of the SAR outlet is impacted by a storm sewer drain that discharges to that side of the river. The remarkable degree of variability in fecal indicator bacteria concentrations over the river mouth, coupled with temporal and spatial variability associated with the surf zone entrainment of ebb flow from the SAR and TM tidal outlets (see section 3.2.1.1), significantly complicates the development of ac-

curate estimates for the mass of fecal indicator bacteria entrained in the surf zone from tidal outlets.

[32] Another complication documented here is that different groups of fecal indicator bacteria exhibit different spatio-temporal patterns in the surf zone, suggesting the existence of multiple sources, and/or multiple transport pathways, for the different indicator groups. As noted elsewhere [Kim *et al.*, 2004; Noble and Xu, 2004], the spatio-temporal distributions of TC concentrations in the surf zone are largely consistent with the notion that, during the field experiment in July 2001, TC were entrained in the surf zone from the SAR and/or TM outlets during ebb tides, and then propagated up-coast at an average velocity not too different from the 0.3 m/s velocity observed during the first dye injection from the TM outlet (compare red streak of TC contamination with diagonal line in Figure 3). Up-coast propagation of the EC and ENT plumes is less obvious; indeed, in several cases these fecal indicator bacteria groups appear to arrive simultaneously at all stations up-coast of the SAR and TM outlets (e.g., ENT event just after midnight, 00:00 to 06:00, on 7/7) as noted by Rosenfeld *et al.* (submitted manuscript, 2005).

[33] Several hypotheses can be formulated to explain the different spatio-temporal patterns observed for TC, on the one hand, and EC and ENT, on the other hand. Hypothesis 3: All fecal indicator bacteria in the surf zone at Huntington Beach originate from a single source (i.e., ebb flow from the SAR and TM outlets), but these bacteria experience multiple fate and transport pathways in the ocean which, when superposed, give rise to the different spatiotemporal patterns evident in Figure 3. Hypothesis 4: There are multiple spatially distinct sources of fecal indicator bacteria in the surf zone at Huntington Beach (in addition to the SAR and TM outlets), and these different sources are characterized by different TC/EC and EC/ENT ratios. In the next several sections we quantitatively analyze the data presented in Figure 3, with the twin goals of better characterizing the along-shore and cross-shore transport processes, and testing the two hypotheses (Hypotheses 3 and 4) articulated above.

**3.2.2.2. Fecal Indicator Bacteria Mass and Cross-Shore Flux of Surf Zone Water**

[34] The top panel in Figure 4 is a plot of the total mass  $M$  of fecal indicator bacteria that flowed out of the SAR and TM outlets, and flowed up-coast past surf zone stations 3N through 15N, during the forty-eight hour study in July 2001. To obtain these bacterial mass estimates, we used an approach similar to the one described above for the dye data (see equation (2), section 3.2.1.3); details of the method employed can be found at the end of this section. Comparing the total mass of bacteria flowing into the ocean during ebb tides from the two outlets (left-most data points, top panel, Figure 4), we find that SAR is a larger source of TC, TM is a larger source of ENT, and both outlets discharge approximately equivalent amounts of EC. The observation that TM is a significant source of ENT is consistent with an earlier study that identified the Talbert Marsh, and its associated flood control channels, as a source of ENT in the surf zone at Huntington Beach [Grant *et al.*, 2001].

[35] The TM and SAR outlets appear to be the primary sources of TC pollution in the surf zone at Huntington Beach. This conclusion is supported by two lines of evidence (top panel of Figure 4): 1. Over the 48 h period

of observation, more TC mass was discharged into the ocean from the TM and SAR outlets than flowed past the surf zone stations at Huntington Beach over the same period of time. 2. The mass of TC flowing past the surf zone stations decays monotonically with distance up-coast of the TM and SAR outlets. Interestingly, the monotonic decay of TC mass in the surf zone appears to be exponential in nature—i.e., the TC mass data all fall along a line when plotted in a log-linear format, see black line in Figure 4. This exponential decay of TC mass with along-shore distance is consistent with the predictions of the simple surf zone transport model presented earlier (equation (3), see also section 4.2.1 for the conditions under which this simple model applies). Indeed, according to this simple transport model, the ratio of the cross-shore and along-shore flux of surf zone water can be estimated from the slope  $m$  of the line formed by plotting log-transformed TC mass  $M(y)$  against along-shore distance  $y$ :

$$\frac{F_c}{F_l} = \frac{-2.303mx_w}{2} \quad (5)$$

The factor 2.303 in equation (5) applies when, as in our case, a base 10 logarithm is used to transform the  $M(y)$  data. Substituting into equation (5) the slope of the black line in Figure 4,  $m = -5.73 \times 10^{-5}/\text{m}$ , and taking  $x_w = 50$  m for the width of the well-mixed region of the surf zone (see section 3.2.1.3), we estimate that  $F_c/F_l = 0.003$ , which is equivalent to  $F_c = 10^{-3}$  m/s for a choice of  $F_l = 0.3$  m/s. This estimate for  $F_c$ , which assumes that bacterial loss from the surf zone is caused solely by cross-shore transport and not bacterial die-off, is approximately 6 fold smaller than the upper-bound estimated from the dye experiments ( $F_c < 0.006$  m/s), and 300 times less than our estimate for the along-shore flux ( $F_l = 0.3$  m/s). Because bacterial die-off may also contribute to the removal of TC from the surf zone, this latest estimate for the cross-shore flux should also be regarded as an upper-bound; i.e.,  $F_c < 10^{-3}$  m/s.

[36] Based on the results presented in Figure 4, the SAR and TM outlets do not appear to be the primary sources of EC and ENT in the surf zone at Huntington Beach. This conclusion is supported by two observations: 1. More EC and ENT mass flowed past the surf zone stations over the 48 h experiment than were discharged from the TM and SAR outlets over the same period of time. 2. The mass of EC and ENT flowing past the surf zone stations does not decay monotonically with distance up-coast of the SAR and TM outlets (as was observed for TC), but rather peaks farther to the north around surf zone station 6N (blue and red points in top panel, Figure 4). Intriguingly, the mass of EC and ENT appears to decay exponentially with distance up-coast of station 6N (i.e., the mass data approximately follow a linear trend in the log-linear plot format used in Figure 4, see blue and red lines). Substituting the slopes of the blue and red lines into equation (5) ( $m = -1.5 \times 10^{-4}/\text{m}$  and  $-1.0 \times 10^{-4}/\text{m}$ , respectively), and taking  $F_l = 0.3$  m/s and  $x_w = 50$  m, the following estimates for the cross-shore volumetric flux are obtained:  $F_c = 3 \times 10^{-3}$  and  $2 \times 10^{-3}$  m/s. Despite the different apparent sources and/or transport pathways of TC, on the one hand, and EC and ENT, on the other hand, once these bacteria are entrained in the surf zone they appear to be removed by cross-shore exchange (and/or die-off) at approx-

imately the same rate (i.e., all estimates of  $F_c$  obtained from the fecal indicator bacteria data agree within a factor of three). Die-off is considered in detail in section 4 of this paper, where we test an unsteady model of fecal indicator bacteria fate and transport in the surf zone that accounts for solar-modulated die-off rates.

[37] The bacterial mass values plotted in Figure 4 were calculated as follows. The mass of bacteria flowing past each surf zone station was calculated from equation (2), substituting hourly measurements of fecal indicator bacteria concentration in the surf zone for  $C(y)$ , letting  $\Delta t = 1$  h, and using the same value estimated earlier for the along-shore volumetric flow rate,  $F_l A_c \approx 8$  m<sup>3</sup>/s (section 3.2.1.3). The mass of bacteria released to the ocean from the SAR and TM outlets was estimated by summing the product  $CQ\Delta t$  over the 48 h experiment, where  $C$  is the concentration of fecal indicator bacteria measured in the SAR or TM outlets (at stations W1, W2, and W3, see Figure 1),  $Q$  is the volumetric flow of water (units m<sup>3</sup>/s) out of the SAR or TM outlets during ebb tides, and  $\Delta t = 1$  h is the sampling interval. The tidal flow of water out of the SAR or TM outlets was estimated from a rating curve as follows:  $Q = vA(l)$ , where  $v$  is the velocity of tidal flow in and out of the outlet (measured using acoustic Doppler velocimeters), and  $A(l)$  represents the wetted cross-sectional area estimated from measured water depth  $l$  (see Grant *et al.* [2002] for details). The concentration  $C$  in the SAR outlet was taken as the mean of all four measurements collected there every hour (i.e., the mean of concentrations measured in samples collected from the top and bottom of the water column at stations W2 and W3).

### 3.2.2.3. TC/EC and EC/ENT Ratios

[38] Geldreich [1976] suggested that the TC/FC and FC/ENT ratios might indicate whether fecal pollution in recreational waters is derived from human or non-human fecal material. Here, FC represents fecal coliform bacteria, a sub-group of TC that includes EC [see Bartram and Reese, 2000]. More recently, Haile *et al.* [1999] reported that human exposure to marine recreational waters in southern California harboring high TC concentrations (>1000) and low TC/FC ratios (<10) might be associated with elevated risk of developing gastrointestinal disease. In practice, interpretation of these ratios is complicated by the fact that different groups of fecal indicator bacteria die-off at different rates in the marine environment: 1. TC die-off faster than FC and EC; and 2. FC and EC die-off faster than ENT [Bartram and Reese, 2000; Sinton *et al.*, 1999]. Because FC and EC are sub-groups of TC, TC/FC and TC/EC ratios should not fall below unity.

[39] Average TC/EC and EC/ENT ratios were calculated from fecal indicator bacteria measurements collected at Huntington Beach over the 48 h sampling period from noon on 5 July to noon on 7 July (2001). The resulting along-shore distribution of these two ratios is displayed in Figure 4 (bottom two panels). The average TC/EC ratio is highest at the SAR outlet, and lower at the TM outlet and in the surf zone, although the standard deviations are large in all cases. The average EC/ENT ratio is highest at the SAR and TM outlets, and lower in the surf zone. The region around 6N—which exhibits the highest along-shore mass of EC and ENT (see top panel in Figure 4, and discussion in the last section)—is anomalous only with respect to the TC/EC



may trigger cases of human illness [Haile *et al.*, 1999; Turbow *et al.*, 2003]. An additional benefit of focusing on the well-mixed portion of the surf zone is that pollutant transport can be treated as a one-dimensional problem; i.e., the pollutant concentration  $C(y, t)$  depends only on time  $t$  and the spatial coordinate  $y$ .

#### 4.1.2. Pollutant Transport in the Surf Zone: Model Derivation and Solution

[45] Here we derive and solve a mathematical model of pollutant transport in the surf zone that is based on the conceptual model described in the last section. In particular, the model accounts for pollutant transport parallel to shore by the along-shore advection, pollutant mixing and stretching in the along-shore direction by longitudinal dispersion and/or turbulent diffusion, and loss from the surf zone by time-dependent reaction and time-dependent cross-shore exchange. These processes can be represented by the following partial differential equation [Kim, 2004]:

$$\frac{\partial C}{\partial t} = -\frac{\partial}{\partial y} \left[ F_l C - D_{eff} \frac{\partial C}{\partial y} \right] - k_{eff} C \quad 0 < x < x_w \quad (6a)$$

$$k_{eff} = \frac{2F_c}{x_w} + k \quad (6b)$$

$$D_{eff} = \varepsilon + D_L \quad (6c)$$

[46] According to equation (6a)—which is a mathematical statement of pollutant mass conservation over the thin slice of the surf zone represented by the inset in Figure 5—the time rate of change of the pollutant concentration  $C$  (units M/T) in the surf zone slice (left hand side of equation (6a)) is equal to the along-shore gradient in the flux of pollutant mass through the surf zone slice due to along-shore advection and diffusive spreading (first term on right hand side) and loss of pollutant mass from the surf zone slice by cross-shore currents and reaction (second term). All variables appearing in these equations were defined earlier in this paper (see Table 2).

[47] Given suitable initial and boundary conditions, equation (6a) can be solved to yield the temporal and spatial distribution of pollutant concentration in the surf zone. In general, pollutants enter the surf zone at multiple locations along the shoreline (e.g., at different tidal outlets). Further, the amount of pollutants entering the surf zone at a particular shoreline location will vary over time due to, at a minimum, the tidal nature of flow in and out of the outlets. To account for this spatial and temporal variability, we proceed in two steps: 1. equation (6a) is first solved for a single slug of pollutant released at a specific time ( $t = t_i$ ) and place ( $y = y_j$ ) along the shore to yield a “fundamental solution” for the  $(i, j)$ th slug. 2. Multiple fundamental solutions are added together, or superposed, to account for the time-varying nature of pollution input from all sources along the shoreline.

[48] Each pollutant slug is uniquely identified by two indices ( $i$  and  $j$ ) and characterized by three physical quantities: its source strength  $M_{i,j}$  (units M/L<sup>2</sup>), its time of release ( $t = t_i$ ), and where it was released along the shore ( $y = y_j$ ).

The corresponding initial and boundary conditions for the  $(i, j)$ th slug become:

$$C(y, t < t_i) = 0 \quad (7a)$$

$$C(y = y_j, t = t_i) = M_{i,j} \delta(y - y_j) \quad (7b)$$

$$C \rightarrow 0 \text{ as } y \rightarrow \pm\infty \quad (7c)$$

$$\partial C / \partial y \rightarrow 0 \text{ as } y \rightarrow \pm\infty \quad (7d)$$

where  $\delta(y)$  (units 1/L) is Dirac’s delta function.

[49] For this set of initial and boundary conditions, equation (6a) can be solved exactly, provided that  $F_l$  and  $D_{eff}$  are fixed constants and  $k_{eff}(t)$  is a function of time only. The resulting fundamental solution for the  $(i, j)$ th slug is [Fischer *et al.*, 1979]:

$$\begin{aligned} C_{slug}(y, t, y_j, t_i, M_{i,j}) &= \frac{M_{i,j}}{\sqrt{4\pi D_{eff}(t - t_i)}} \\ &\cdot \text{Exp} \left( -\frac{[(y - y_j) - F_l(t - t_i)]^2}{4D_{eff}(t - t_i)} - \int_{t_i}^t k_{eff}(\zeta) d\zeta \right) \\ &0 < x < x_w, \quad t > t_i \end{aligned} \quad (8)$$

[50] As written, this solution corresponds to the case where the surf zone is initially clean, and then at time  $t = t_i$  a single slug of pollutant from a point source located at  $y = y_j$  is instantaneously mixed into the cross-sectional area  $A_c$ . Using the Principle of Linear Superposition [Fischer *et al.*, 1979], the time-varying input of pollutants from a single tidal outlet located at  $y = y_j$  can be approximated by summing up a series of slugs separated in time by  $\Delta t$ , where  $\Delta t$  is small compared to the period of a single ebb tide; i.e.,  $\Delta t \ll 6$  h:

$$C_{outlet}(y, t, j) = \sum_{i=0}^{t/\Delta t} C_{slug}(y, t, y_j, t_i = i\Delta t, M_{i,j}) \quad (9)$$

The contribution of multiple tidal outlets to surf zone contamination can be found by summing equation (9) over all tidal outlets ( $j = 1$  to  $N$ ):

$$C(y, t) = \sum_{j=1}^N C_{outlet}(y, t, j) \quad (10)$$

The source strength of the  $(i, j)$ th slug is

$$M_{i,j} = \alpha_{i,j} C_{i,j}(t = i\Delta t) Q_{i,j}(t = i\Delta t) \Delta t / A_c, \quad Q_{i,j} > 0 \quad (11a)$$

$$M_{i,j} \equiv 0, \quad Q_{i,j} \leq 0 \quad (11b)$$

where  $Q_{i,j}$  represents the volumetric flow rate (in units of L<sup>3</sup>/T) of water in ( $Q_{i,j} < 0$ ) or out ( $Q_{i,j} > 0$ ) of the  $j$ th outlet at

the  $i$ th time, and  $\alpha_{ij}$  represents the fraction of the tidal effluent which is entrained into the surf zone from the  $j$ th outlet at the  $i$ th time (see Figure 5 for a graphical representation of these quantities).

#### 4.1.3. Pollutant Transport in the Surf Zone: Parameter Estimation

[51] To compare model predictions with observed fecal indicator bacteria concentrations in the surf zone, model simulations were carried out for the same 48 h period covered by the 6–7 July 2001 field experiment (see Figure 3). To model this experiment, we used parameter values that were either known ( $N = 2$  for the two tidal outlets,  $y_{TM} = 300$  m and  $y_{SAR} = 0$  m for the location of the TM and SAR outlets,  $\Delta t = 1$  h for the sampling rate of fecal indicator bacteria concentrations and tidal flow rates in the TM and SAR outlets), or estimated for this period of time ( $F_l = 0.3$  m/s,  $F_c = 10^{-3}$  m/s, section 3.2.2.2), or estimated from dye experiments carried out under similar wave conditions ( $D_{eff} = 40$  m<sup>2</sup>/s, and  $x_w = 50$  m,  $h_w = 1$  m, sections 3.2.1.1 and 3.2.1.3) (see Table 2).

[52] Based on an analysis of the dye and fecal indicator bacteria data described in section 3, the parameters  $F_l$ ,  $F_c$ ,  $D_{eff}$ , and  $x_w$  are relatively stable, within a factor of three or better. Because  $h_w$  depends on  $x_w$  through the beach slope—which is not expected to vary much over the time scale of our field experiments—the former parameter should also be relatively stable. The parameter that is likely to be the most variable, and about which the least is known, is the fraction  $\alpha_{SAR}$  and  $\alpha_{TM}$  of tidal flow from the SAR and TM outlets that is entrained in the surf zone. Dye results presented earlier suggest this parameter is highly variable, both at different outlets for a fixed time, and at the same outlet for different times (see section 3.2.1.1). For the calculations presented below, these two parameters were estimated by finding values that minimized the least-squares difference between the predicted and measured TC concentration at surf zone station 3N. The TC signal at 3N was chosen because: 1. This surf zone station is nearest the tidal outlets, and hence water quality at this site is the most likely to be influenced by bacteria flowing out of the outlets during ebb tides. 2. All available evidence supports the idea that the SAR and TM outlets are significant sources of TC in the surf zone at Huntington Beach (section 3.2.2).

[53] Finally, to account for the sunlight modulated die-off of fecal indicator bacteria (the  $k$  term in equation (6b)), first-order decay was written [Sinton *et al.*, 1999]:

$$k(t) = k_{FIB}I(t) \quad (12)$$

where  $I(t)$  and  $k_{FIB}$  represent, respectively, measured sunlight irradiation (in units of W/m<sup>2</sup>) and fecal indicator bacteria die-off rate constant (in m<sup>2</sup>/Whr). Hourly measurements of total incoming solar radiation (Kipp and Zonen, CM3 Thermopile Radiometer, The Netherlands) in the nearby San Joaquin marsh were substituted for  $I(t)$ , and the following values were employed for the die-off rate constant of the different fecal indicator bacteria groups [Sinton *et al.*, 1999]:  $k_{TC} = 1.8 \times 10^{-3}$ ,  $k_{FC} = 1.7 \times 10^{-3}$ , and  $k_{ENT} = 9.7 \times 10^{-4}$  m<sup>2</sup>/Whr.

#### 4.1.4. Modeling Wave-Driven Along-Shore Currents

[54] Deep water wave data were monitored during the 5–7 July 2001 fecal indicator bacteria experiment by the CDIP

San Pedro Buoy [CDIP, 2003], Station #092, moored offshore near Huntington Beach at 33 37.070 N, 118 19.020 W where the local water depth is 457 m. The CDIP buoy data was reprocessed to yield time series (with a 30 min sampling rate) of deep water significant wave height, period and direction. These data were then used to drive the wave refraction model; specifically, waves measured at the offshore buoy were shoaled onto a 31 km reach of surf zone centered on SAR outlet. The shoaling computations were performed on a 200 × 400 point rectangular grid (3 arc-second grid cell resolution) using a refraction/diffraction code based on the parabolic equation method applied to the mild slope equations for surface gravity waves [Kirby, 1986; O'Reilly and Guza, 1991]. These shoaling computations produced estimates of breaker heights  $H_b$  and angles  $a_b$  at 30-minute intervals for each 120 m increment of shoreline within the wave shoaling grid. Breaker heights were calculated from stepwise refraction/diffraction computations by solving for the grid cells in which the local shoaling wave height matches the depth dependent breaker criteria [Raubenheimer and Guza, 1996],  $H_b = \gamma h_b$ , where  $h_b$  is the depth of wave breaking and  $\gamma = 0.78$ . The suite of local solutions for  $(H_b, a_b, h_b, T)$  allow computations of the components of the break point radiation stress tensor [Longuet-Higgins and Stewart, 1964], from which the along shore current profiles,  $v_l(x, y, t)$ , were calculated at each 120 m shoreline increment using the Bowen formulation [Bowen, 1969]. These calculations assumed a uniform mean beach slope  $\tan \beta = 0.02$ , and a  $K$ -factor relating the position of maximum set-up to the still-water line of  $K = 0.4$ .

## 4.2. Results

### 4.2.1. Exponential Along-Shore Decay in Pollutant Mass

[55] In section 3.2.2.2 we noted that the mass of fecal indicator bacteria flowing past a particular surf zone station appears to decay exponentially with along-shore distance from the source of contamination (either the SAR or TM outlet, or a source farther to the north around surf zone station 9N). The exponential decline of surf zone pollution with along-shore distance has been observed elsewhere [Inman *et al.*, 1971; J. Largier, personal communication] and justified theoretically using steady-state tanks-in-series [Inman *et al.*, 1971] and differential equation [Boehm, 2003] models of surf zone transport and dilution; indeed, the steady-state solution to the Boehm model is presented as equation (3) earlier in this paper. However, it is not clear if steady-state models are a valid approximation of the highly unsteady conditions that prevail in the surf zone. Further, these previous models focus on the decay of pollutant concentration with along-shore distance—whereas the present study is concerned with the decay of pollutant mass with along-shore distance—and they do not consider along-shore transport of mass in the surf zone by longitudinal dispersion and/or turbulent diffusion, where the latter could be important under certain conditions (e.g., when the waves break with their crests parallel to the beach). In this section we identify the conditions under which simple steady-state expressions—like equation (3)—can be used to interpret pollutant or tracer measurements in the surf zone.

[56] As was the case for the experimental observations described earlier in this paper (sections 3.2.1.3 and 3.2.2.2),

we imagine that an observer measures pollutant or tracer concentration in the surf zone at a fixed position  $y$  along the shoreline for a long period of time (approximated here as  $t \rightarrow \infty$ ). Over this period of observation, the total mass of tracer or pollutant flowing parallel to the shore can be written thus:

$$M(y) = \int_0^{\infty} C(y, t) F_l A_c dt \quad (13)$$

[57] We are specifically interested in understanding the mass-distance relationships predicted by equation (13) for the case where concentrations in the surf zone vary with time. Accordingly we utilized our solution (equation (8)) for the case where pollutant mass is added to the surf zone in a pulse and, from there, undergoes along-shore advection, along-shore dispersion (and/or turbulent diffusion), cross-shore dilution, and first-order decay. Combining equations (8) and (13), and evaluating the resulting integral, we arrive at the following expression for the total mass of pollutant measured in the surf zone a distance  $y$  down-current from the source:

$$M(y) = \frac{M_{i,j}}{\sqrt{1+Br}} e^{-Pe(\sqrt{1+Br}-1)/2} \quad (14a)$$

$$Pe = \frac{F_l y}{D_{eff}} \quad (14b)$$

$$Br = \frac{4 k_{eff} D_{eff}}{F_l^2} \quad (14c)$$

The same expression applies for the case where multiple pulses are released from the same location (at  $y = 0$ ), only in that case  $M_{i,j} \rightarrow M_T$ , where  $M_T$  is the total mass released over multiple pulses. The Peclet number ( $Pe$ ) represents the relative importance of advective and dispersive (or diffusive) transport. The Brooks number ( $Br$ , so named in honor of Norman Brooks, Emeritus Professor at Caltech) represents the relative influence of along-shore transport by advection and dispersion (or turbulent diffusion) and removal from the surf zone by cross-shore currents and/or first-order decay.

[58] Both the unsteady and steady-state models predict that  $M = a M_{i,j} e^{-by}$  (compare equations (3) and (14a)). However, these two models predict different expressions for the constants  $a$  and  $b$ . Specifically, the steady-state model (equation (3)) predicts that  $a = 1$  and  $b = k_{eff}/F_l$ , whereas the unsteady model (equation (14a)) predicts that  $a = 1/\sqrt{1+Br}$  and  $b = F_l(\sqrt{1+Br} - 1)/2D_{eff}$ .

[59] The unsteady model constants converge to the steady-state model constants provided that  $Br \ll 1$  (to show this result for the constant  $b$  one needs to use the power expansion approximation  $\sqrt{1+x} \approx 1 + x/2$  for  $x \ll 1$ ). In the other limit ( $Br \gg 1$ ), the unsteady model constants converge to a different set of expressions:  $a = F_l/2 \sqrt{k_{eff} D_{eff}}$  and  $b = \sqrt{k_{eff}/D_{eff}} - F_l/2D_{eff}$ . These two limits correspond to the physical situations where along-

shore advection exerts a strong ( $Br \ll 1$ ) or weak ( $Br \gg 1$ ) influence on pollutant fate and transport in the surf zone. Using the set of parameter values estimated from the dye and fecal indicator bacteria studies reported earlier (see Table 2),  $Br \approx 0.1$ . Hence, to a good approximation, the simple steady-state model for the decay of mass with along-shore distance (equation (3)) should be valid for the unsteady and advectively dominated transport conditions that prevailed during the field experiments reported in this paper.

#### 4.2.2. Observed and Model-Predicted Fecal Indicator Bacteria Concentrations

[60] In this section we use the unsteady model derived in section 4.1.2 to simulate fecal indicator bacteria concentrations in the surf zone at Huntington Beach (between stations 3N to 15N). These model simulations were carried out under the following assumptions: 1. All fecal indicator bacteria in the surf zone at Huntington Beach originate solely from the TM and SAR outlets. 2. The fate and transport of fecal indicator bacteria in the surf zone is controlled by along-shore advection, longitudinal dispersion, cross-shore dilution, and solar modulated die-off.

[61] The model predicted concentrations, together with actual measurements of fecal indicator bacteria concentrations, are presented in Figure 6. The first row of panels in the figure depict water level measured at the TM outlet and sunlight intensity measured in the nearby San Joaquin marsh; periods of rising tide are represented by a set of blue vertical stripes. The second row of panels in Figure 6 depicts the measured concentration of fecal indicator bacteria at the SAR (solid line) and TM (dashed line) outlets approximately 100 m inland of where water from the outlets flows into the ocean. The concentration of fecal indicator bacteria in the SAR and TM outlets is set to zero during flood tides, when water is flowing into the outlet from the ocean, as indicated by Doppler velocimeters installed at the two outlets [Kim *et al.*, 2004] (note that during the small rising tide on 7/6 the ebb flow slowed but did not reverse direction). The SAR curve represents the mean of the four measurements carried out at stations W1 and W2 every hour.

[62] The remaining rows in Figure 6 depict the observed (black line) and predicted (colored lines) concentration of fecal indicator bacteria at surf zone stations, in order from down-coast to up-coast: 3N (third row), 6N (fourth row), 9N (fifth row), 12N (sixth row), and 15N (seventh row). The fecal indicator bacteria data plotted in this figure are the same as those presented in Figure 3. Again, it is important to emphasize that these model predictions take, as input, hourly measurements of fecal indicator bacteria loading into the ocean from the SAR and TM outlets, hourly measurements of solar radiation, and the set of parameter values listed in Table 2. Three limiting cases of the model are considered: 1. Advection, dispersion, cross-shore mass loss, and sunlight modulated die-off reaction all influence the fate and transport of fecal indicator bacteria in the surf zone (referred to here as the ADMR model, red lines in the figure). 2. Reaction is neglected (ADM model, blue lines). 3. Both reaction and mass-loss by cross-shore exchange are neglected (AD model, yellow lines).

[63] As expected, the model predicted concentrations increase in the order ADMR < ADM < AD. Prior to

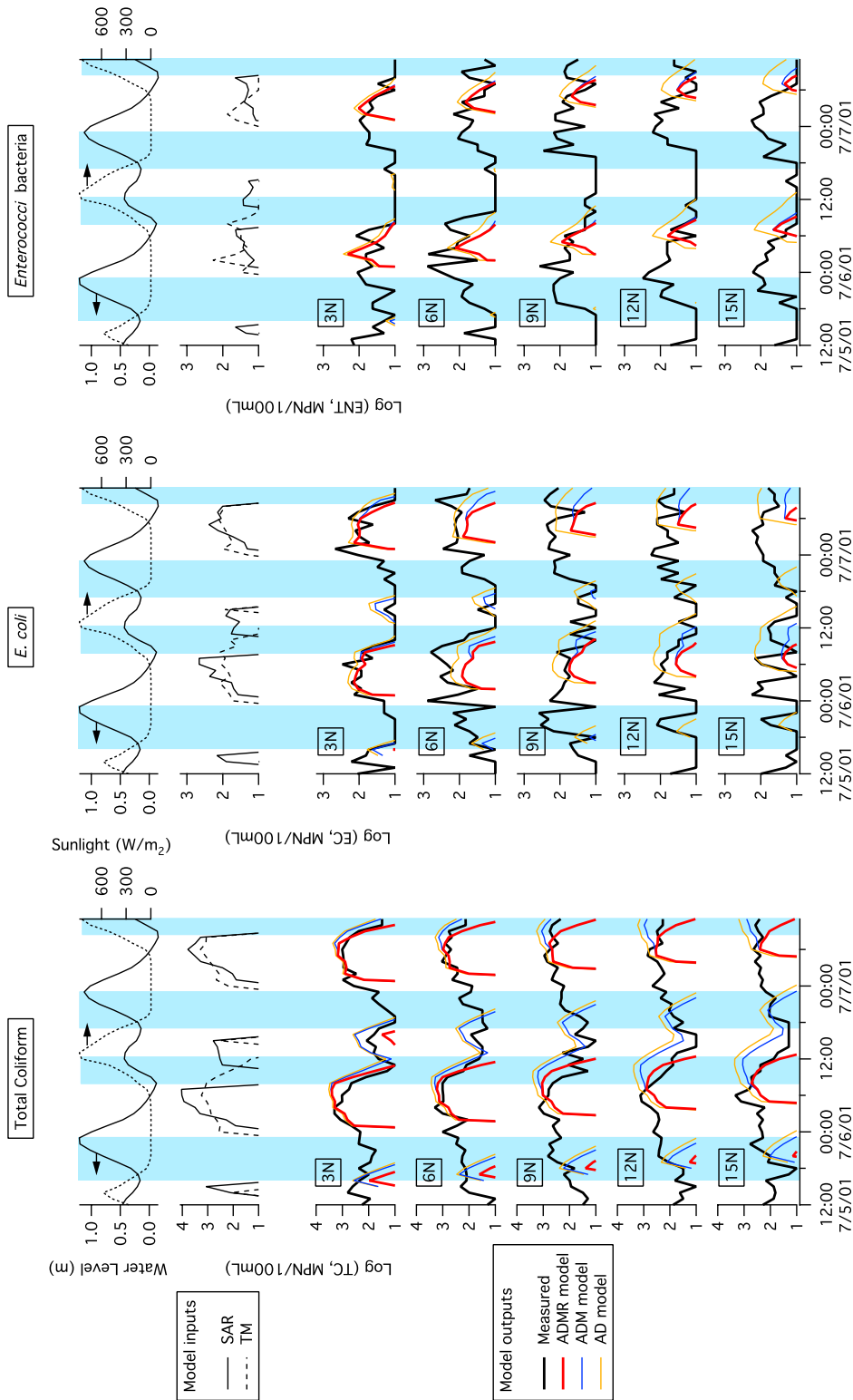


**Figure 6.** Measurements and model predictions of fecal pollution in the surf zone at Huntington Beach on 5–7 July, 2001. Top row: mean sea level measured at the TM outlet and sunlight intensity measured in the nearby San Joaquin Marsh. Second row: concentrations of fecal indicator bacteria at the Santa Ana River and the Talbert Marsh (dashed line) outlets (note that in this plot the concentrations are set to zero during flood tides). Third–seventh row: model-predicted and observed fecal indicator bacteria concentrations at surf zone stations 3N, 6N, 9N, 12N, and 15N. The solid black line represents measured data, and the colored lines represent predictions of the ADMR (red), the ADM (blue), and the AD (yellow) models. Blue vertical stripes indicate periods of rising tide.

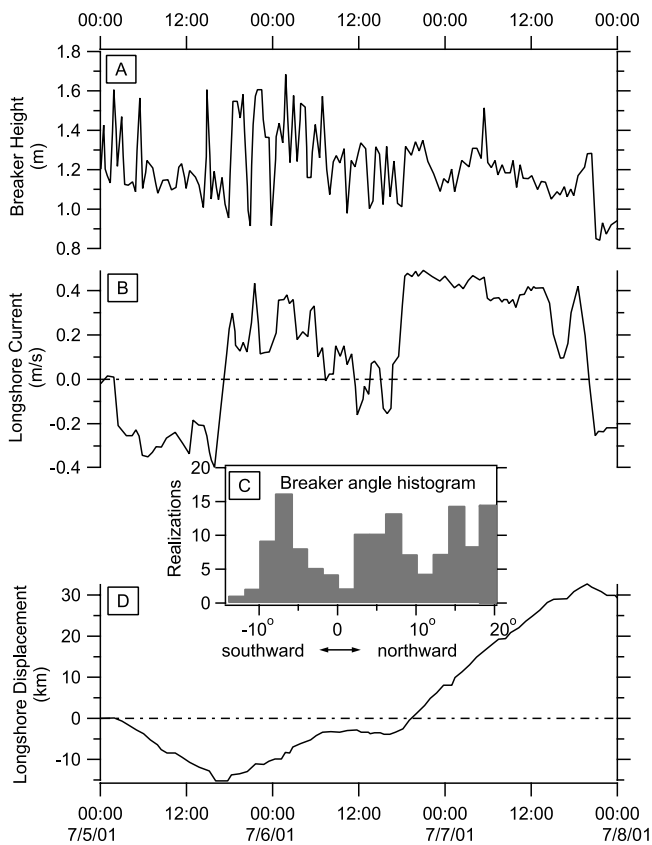


**Figure 7.** (a) Breaker height, (b) longshore current at  $x_w = 50$  m, (c) histogram of breaker angle, and (d) alongshore drift displacement from station 0 at the Santa Ana River mouth. Negative currents resulting from negative breaker angles flow downcoast to the south (wave data refracted from CDIP San Pedro Buoy, #092).

midnight on 7/6, all three models under-predict observed concentrations of fecal indicator bacteria in the surf zone. This result is a consequence of “start-up effects”, which arise from the finite nature of the time series measurements at the SAR and TM outlets, together with the model assumption that the surf zone is initially free of fecal pollution (see section 4.1.2). In general, the difference between the ADMR and ADM curves is most pronounced during the daytime, when solar radiation levels cause significant bacterial die-off.

[64] After midnight on 7/6, the AD and ADM models correctly predict two TC and EC pulses per day at 3N (first and second columns of plots); however, the ADMR model significantly under-predicts the smaller of these two pulses. All three models appear to capture the up-coast propagation of the larger TC pulses, and the two models that neglect sunlight-induced die-off (AD and ADM) appear to predict the up-coast propagation of the smaller TC pulse as well. Post midnight 7/6, all three models predict the tidal cycling of EC at 3N (second column of plots); however they significantly under-predict EC concentrations measured farther up-coast. At stations 6N and 9N, the concentration of EC is high during flood tides when the model predicts that EC concentrations should be low. All three models significantly under-predict the concentration of ENT at all

of the surf zone stations, particularly those up-coast of 3N (third column of plots).

[65] Overall, the ADMR model does a reasonable job of predicting TC, and to a lesser extent EC, occurrence patterns in the surf zone at Huntington Beach. However, the model does a poor job of predicting ENT concentrations in the surf zone, suggesting that there must be additional sources of, and/or transport pathways for, this latter group of fecal indicator bacteria. The timing of ENT pulses suggests that these bacteria are supplied to the surf zone during large flood tides. In this regard, it is interesting to note that, during the dye experiments on 1 May 2000, dye seaward of the surf zone recycled back into the surf zone over several days, and this re-introduction of dye into the surf zone appeared to peak during flood tides. Together, these two observations are consistent with Hypothesis 3 which envisioned two transport pathways for fecal indicator bacteria at our field site: direct entrainment into the surf zone, plus transport offshore followed by recycling back into the surf zone.

#### 4.2.3. Wave-Driven Along-Shore Currents at Huntington Beach

[66] In this section we present modeling studies of wave-driven currents in the surf zone at Huntington Beach over the period of time when the field measurements of fecal indicator bacteria, described above, were carried out. These calculations provide insights into the origin of near-shore currents at Huntington Beach, and provide a theoretical justification for the recurrent observation that pollutants (dye and bacteria) were transported parallel to shore at about 0.3 m/s during the field experiments reported here.

[67] Figure 7 presents model-predicted time series of breaking wave height and angle at the SAR outlet (panels A and C, respectively) over the 48 h period when fecal indicator bacteria were measured hourly in the surf zone. Model predictions of wave height at noon on 7 July are illustrated in Figure 8. The middle panel in Figure 7 is a plot of the temporal variability of the predicted along-shore current during the July 2001 experiment. The along-shore current at station 0 (at the SAR outlet) is evaluated at a distance  $x = x_w = 50$  m where the local water depth is  $h_w = 1$  m (currents flowing northward toward Huntington Beach from the SAR are given a positive sign).

[68] The lower panel in Figure 7 is a plot of the along-shore displacement of a particle based on the lowest order approximation to Lagrangian mean drift [Longuet-Higgins, 1953], derived from gradients and time integration of  $v_j(x, y, t)$  at  $x = x_w$ . Inspection of the along-shore current and displacement time series in Figure 7 indicates that a net up-coast along-shore drift away from SAR and toward Huntington Beach began on the afternoon of 5 July 2001, and continued until late in the day on 7 July 2001. This up-coast drift coincided with the arrival of a south swell from  $190^\circ$  which initially brought intermittent forerunners with periods of  $T = 16$  sec, and breakers of  $H_b = 1.4\text{--}1.6$  m [CDIP, 2003]. These forerunners had group intervals comparable to those first observed in Southern California by Snodgras *et al.* [1966], and the southern obliquity ( $190^\circ$ ) suggests similar Southern Hemisphere origin. The forerunner groups arrived about 30 minutes to 1.5 hours apart and continued from the afternoon of 5 July until the afternoon of 6 July, during which time the along-shore current would

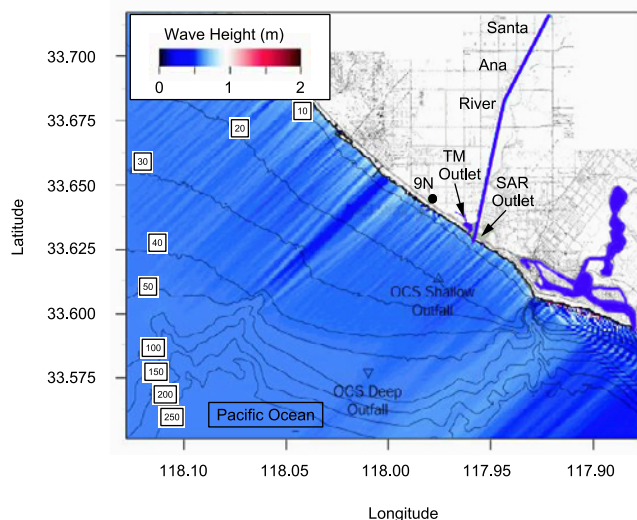


**Figure 8.** Refraction/diffraction pattern of wave field at 12:03 hours on 7 July 2001 during the dispersion study of fecal indicator organisms in the neighborhood of the Santa Ana River and Huntington Beach. Incident wave height equal to 0.60 m, period equal to 9.09 s, direction equal to  $190^\circ$  (from CDIP, San Pedro Buoy, Station #092).

pulsate with the arrival of each forerunner group. A continuous, steady south swell arrived in the afternoon of 6 July and persisted until the evening of 7 July [CDIP, 2003], with periods of  $T = 9$  s and breaker heights of  $H_b = 1.0$ – $1.2$  m. Because of the steadiness of this swell, the along-shore current remained quasi-steady during this period, with mean velocities varying slowly between 0.30 and 0.45 m/s. The along-shore particle displacement in Figure 7 shows that the mean drift rate over the 48 hour period of the south swell event is 0.27 m/s, consistent with our previous estimates for the along-shore flux of  $F_l = 0.3$  m/s (section 3).

[69] Figure 9 shows the alongshore variability of  $v_y(x, y, t)$  and the divergence of drift  $\partial v_y(x, y, t)/\partial y$ . Both  $v_y(x, y, t)$  and  $\partial v_y(x, y, t)/\partial y$  are evaluated at  $x = x_w$  at mid-day on 7 July 01, when the swell and along-shore current were fairly steady (Figure 7). To avoid spurious end effects of the refraction grid (Figure 8) only 20 km of the 31 km reach of coastline around the SAR are evaluated in Figure 9. Inspection of Figure 9 reveals that the along-shore current flows up-coast at a fairly uniform rate between SAR and 9N, with a mean of about 0.3 m/s. However, immediately north of 9N, the along-shore current slows down. The same type of along-shore variations occurs again immediately up-coast of 15N, and at both locations, the retardation in along-shore current leads to a negative divergence of drift. These non-uniformities in the along-shore currents are induced by the shadows and bright spots in the refraction/diffraction pattern (Figure 8) caused by wave shoaling over irregularities in shelf bathymetry. In particular the large shadow and adjacent bright spots found near the Huntington Beach Pier in Figure 8 are responsible for the large deceleration in along-shore current and negative divergence of drift near station 15N. Negative divergences of drift will probably increase the cross-shore mixing of contaminants into adjacent offshore waters via rip currents [Bowen and Inman, 1969].

[70] In summary, it is probably reasonable to assume that the along-shore drift at Huntington Beach is fairly constant, at least for the July 5–7 (2001) time frame and the particular stretch of surf zone (between the SAR outlet and surf zone station 15N) for which high frequency fecal indicator bacteria measurements are available. The along-shore current was quasi-steady for the period in question, and the mean value of 0.3 m/s agrees closely with particle drift rates calculated from the spatial and temporal variability of the shoaling wave field. However, the spatial non-uniformities that were resolved in the along-shore drift could lead to along-shore variability in the rate at which pollutants are exchanged between the surf zone and offshore. Indeed, the fact that the along-shore current decelerates around 9N and 15N implies that these areas likely experience enhanced cross-shore exchange.

## 5. Summary and Future Prospects

[71] The near shore fate and transport of dye, fecal indicator bacteria and, by inference, other contaminants, from tidal outlets at Huntington Beach appear to involve five distinct processes: 1. Highly variable surf zone entrainment of contaminants discharged to the ocean from tidal outlets during ebb tides. 2. Transport of the contaminants parallel to shore at a velocity  $F_l$  (approximately equal to 0.3 m/s during the experimental realizations described above). 3. Stretching of contaminant plumes parallel to the shore by turbulent diffusion and/or longitudinal dispersion. 4. Permanent removal of contaminants from the surf zone by reaction (solar-modulated die-off in the case fecal

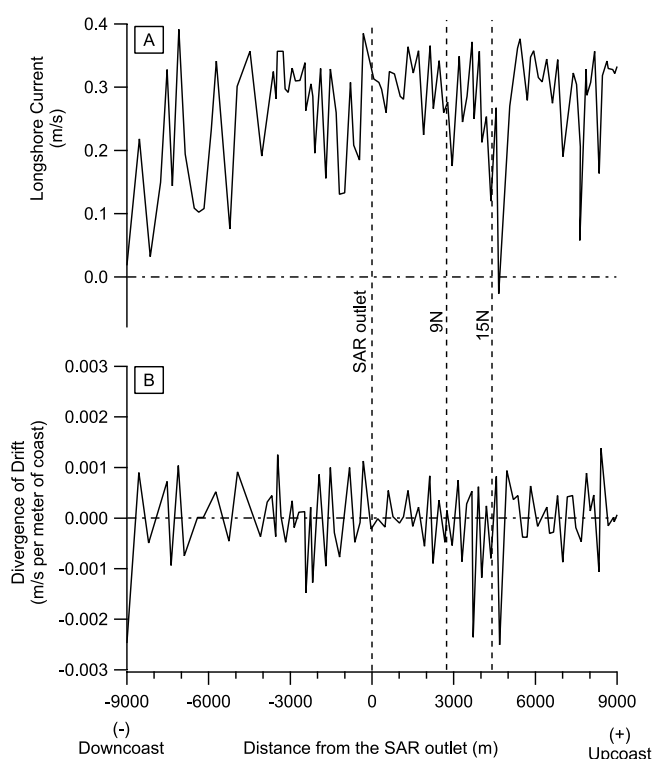


**Figure 9.** Longshore variation of drift for 7 July 2001 at 12:03 hours. (a) Longshore current at  $x_w = 50$  m; (b) divergence of drift at  $x_w = 50$  m.

indicator bacteria) and/or by translation seaward of the surf zone by cross-shore currents. 5. Recycling of contaminants back into the surf zone from offshore—a process which appears to occur preferentially during rising tides.

[72] When waves approach Huntington Beach from the south, the resulting along-shore drift in the surf zone  $F_l$  is approximately 0.3 m/s, based on dye studies, TC measurements in the surf zone, and wave modeling studies. The close agreement between these various experimental and theoretical estimates for the along-shore drift is one of the more remarkable features of this study.

[73] The along-shore volumetric flux of water in the surf zone is orders of magnitude larger than the cross-shore volumetric flux (at least 50 times greater based on the dye data, and at least 300 times greater based on the fecal indicator bacteria data). This last observation is consistent with the areal images presented in Figure 1 that reveal that dye fields quickly become elongated in the along-shore direction at Huntington Beach, at least during the four realizations studied here. In general, along-shore transport, cross-shore transport, longitudinal dispersion, and turbulent diffusion in the surf zone are all likely to be sensitive to local wave conditions (e.g., the angle the wave breaks against the shoreline, and the height of the breaking wave [see *Longuet-Higgins*, 1970a, 1970b]). Indeed, further research into the relationship between these transport parameters and wave conditions seems warranted.

[74] Comparing the rate of removal of fecal indicator bacteria from the surf zone by cross-shore exchange (ca.,  $<10^{-5} \text{ s}^{-1}$ ) and die-off (ca., 0 to  $10^{-4} \text{ s}^{-1}$ ) (see Table 2) suggests that either one (or both) of these processes could be important, depending on solar irradiation levels. Specifically, during periods when solar irradiation is nil (i.e., at night) cross-shore exchange should dominate fecal indicator bacteria removal from the surf zone, whereas when solar irradiation is maximal (i.e., around noon) die-off will likely dominate removal of fecal indicator bacteria from the surf zone. In light of these results, it is interesting to note that the loading of fecal indicator bacteria to the ocean from the SAR and TM outlets peaked during the large midnight ebb tides (see Figure 6). The implication is that cross-shore exchange may have dominated the removal of fecal indicator bacteria from the surf zone at Huntington Beach, at least during the set of field experiments reported here.

[75] The results presented in this study help to constrain possible sources of fecal indicator bacteria pollution in the surf zone at Huntington Beach. Multiple lines of evidence suggest that TC in the surf zone originate from ebb flow out of the SAR and TM outlets. This conclusion is based on the following evidence: 1. The SAR and TM outlets mark the down-coast edge of significant TC and EC pollution in the surf zone. 2. Waves were out of the south to south-west, and hence surf zone currents should have been directed up-coast. 3. Plumes of TC appear to propagate up-coast in the surf zone at approximately 0.3 m/s—the same velocity observed for the propagation of dye in the surf zone under similar wave conditions, and the same velocity predicted by wave refraction modeling of that period of time. 4. The concentration of TC in the surf zone is highest during the large midnight ebb, when water from the SAR and TM flows over the beach and into the ocean. 5. The total mass of TC released from the SAR and TM outlets exceed the total

mass of TC that flowed past up-coast surf zone stations. 6. The total mass of TC flowing past the up-coast surf zone stations declines exponentially with distance up-coast of the SAR and TM outlets.

[76] The occurrence patterns of EC and ENT, on the other hand, are more complex, and reflect either the recycling of fecal indicator bacteria back into the surf zone (Hypothesis 3) or additional sources of these indicator bacteria along the shoreline, particularly in the region around 6N to 9N (Hypothesis 4). Arguments can be made in favor of either of these two hypotheses. Mass calculations support Hypothesis 4, because there appears to be more EC and ENT mass passing the surf zone stations than is released from the TM and/or SAR outlets over the same period of time. However, calculations of total mass released from the outlets may be confounded by the very significant variability of EC and ENT concentration across the SAR outlet, together with the possibility that the average along-shore velocity may not have been 0.3 m/s at all stations (e.g., negative divergence of drift is predicted from radiation stress calculations in the 15N region).

[77] Hypothesis 4 is also consistent with a recently published study that utilized short-lived radium isotopes ( $^{223}\text{Ra}$  and  $^{224}\text{Ra}$ ) to estimate the flux of shallow saline groundwater (SSG) into the surf zone at Huntington Beach [*Boehm et al.*, 2004a, 2004b]. This later study found an association between the flux of SSG into the surf zone (as indicated by radium isotope and nutrient data) and the surf zone concentration of fecal indicator bacteria around stations 6N and 9N. However, all but one of the SSG samples collected had very low concentrations of fecal indicator bacteria, and hence the authors were unable to establish SSG as the source of fecal pollution at this site. In an earlier paper, *Boehm et al.* [2002b] presented evidence that the Orange County Sanitation District's sewage outfall—which discharges partially treated sewage effluent through a submarine outfall located approximately 5 km offshore of the SAR outlet at a depth of approximately 60m—might be a source of fecal contamination in the surf zone at Huntington Beach, by internal wave driven cross-shore transport. Follow-up studies, however, have largely ruled out the sewage outfall as a source of fecal indicator bacteria pollution in the surf zone at Huntington Beach. This conclusion is supported by the fact that the water quality problem in the Huntington Beach surf zone persisted after the District dramatically reduced the concentration of fecal indicator bacteria in their sewage effluent by initiating partial disinfection [*Noble and Xu*, 2004].

[78] On the other hand, Hypothesis 3 is consistent with the timing (during rising tides) of EC and ENT inputs into the surf zone at stations 6N and 9N, and the observation that EC and ENT mass is greatest in the 6N to 9N area, where a thermal plume may increase cross-shore exchange rates. Remarkably, despite the very different spatial patterns of TC, on the one-hand, and EC and ENT, on the other hand, cross-shore exchange rate estimated from all three fecal indicator bacteria groups (TC, EC, and ENT) agree within a factor of 2 to 3.

[79] The field data and modeling results presented in this paper have significant implications for the health of recreational bathers. Surfing, swimming, and other ocean recreation tends to be concentrated very near to shore (inside, or

just outside, of the surf zone)—precisely the same region where near shore currents appear to focus pollution from tidal outlets. The intersection of human recreation and near-shore pollution pathways implies that, from a human health perspective, special care should be taken to reduce the discharge of harmful pollutants from land-side sources of surface water runoff, such as tidal outlets and storm drains.

[80] The field data presented in this study underscore the degree to which the concentration of pollution in the surf zone varies in both space and time. While it is generally understood that fecal pollution concentrations—and hence human health risk from recreational bathing—can vary with along-shore distance from storm drains and other shoreline outfalls [Haile *et al.*, 1999; Pruss, 1998], the influence of temporal variability in pollution concentrations may be less appreciated. That variability includes not only sub-tidal to inter-annual variability evident from analysis of historical water quality records [Boehm *et al.*, 2002a, 2004b; Boehm and Weisberg, 2005], but also hour-to-hour variability that is spatially coherent over multi-kilometer stretches of the shoreline. Given that concentrations of fecal indicator bacteria at a single location in the surf zone can vary by orders of magnitude over a short period of time (ca., 6 h), the human health risk experienced by recreational bathers may be determined as much by when they go into the water, as where they go into the water. The human health implications of temporally and spatially variable concentrations of fecal pollution in the surf zone would appear to be an important avenue of future research—one that will necessitate the cooperation of oceanographers, engineers, and human health experts.

[81] **Acknowledgments.** Data and analysis described in this paper were supported by a grant from the National Water Research Institute (EC 699-632-00), the UC Marine Council (UCMarine-32114), and matching funds and in-kind support from the Orange County Sanitation District, County of Orange, California Department of Parks and Recreation, the Huntington Beach Wetlands Conservancy, and the cities of Huntington Beach, Fountain Valley, Costa Mesa, Santa Ana, and Newport Beach. We gratefully acknowledge the following individuals and institutions for their help with this study: J. Largier, R. Linsky, S. Ensari, B. F. Sanders, C. D. MaGee, Kaiser, L. Waldner, C. Crompton, B. Moore, M. Brill, S. Jiang, L. Grant, H. Johnson, N. Jacobsen, I. Forrest, C. Webb, D. McClain, L. Kirchner, K. Patton, J. Gerdes, M. Yahya, T. Pira, H. Gil, S. Ha, A. Canonizado, A. Doria, B. Manalac, M. Fujita, C. Lin, C. Tse, A. Mojab, A. Ung, G. Kwong, C. Salazar, F. deLeon, A. Rinderknecht, F. Cheng, A. Hilman, and D. Quam.

## References

- Ahn, J. H., S. B. Grant, C. Q. Surbeck, P. M. DiGiacomo, N. P. Nezlín, and S. Jiang (2005), Coastal water quality impact of storm runoff from an urban watershed in southern California, *Environ. Sci. Technol.*, in press.
- Bartram, J., and G. Rees (2000), Monitoring Bathing WATERS: A practical guide to the design and implementation of assessments and monitoring programmes, World Health Org., Geneva.
- Boehm, A. B. (2003), Model of microbial transport and inactivation in the surf zone and application to field measurements of total coliform in Northern Orange County, California, *Environ. Sci. Technol.*, 37(24), 5511–5517.
- Boehm, A. B., and S. B. Weisberg (2005), Tidal forcing of Enterococci at marine recreational beaches at fortnightly and semi-diurnal frequencies, *Environ. Sci. Technol.*, in press.
- Boehm, A. B., S. B. Grant, J. H. Kim, C. D. McGee, S. Mowbray, C. Clark, D. Foley, and D. Wellmann (2002a), Decadal and shorter period variability of surf zone water quality at Huntington Beach, California, *Environ. Sci. Technol.*, 36, 3885–3892.
- Boehm, A. B., B. F. Sanders, and C. D. Winant (2002b), Cross-shelf transport at Huntington Beach: Implications for the fate of sewage discharged through an offshore ocean outfall, *Environ. Sci. Technol.*, 36(9), 1899–1906.
- Boehm, A. B., G. G. Shellenbarger, and A. Paytan (2004a), Groundwater discharge: Potential association with fecal indicator bacteria in the surf zone, *Environ. Sci. Technol.*, 38(13), 3558–3566.
- Boehm, A. B., D. B. Lluh-Cota, K. A. Davis, C. D. Winant, and S. G. Monismith (2004b), Covariation of coastal water temperature and microbial pollution at interannual to tidal periods, *Geophys. Res. Lett.*, 31, L06309, doi:10.1029/2003GL019122.
- Boer, W. F., L. Rydberg, and V. Saide (2000), Tides, tidal currents and their effects on the intertidal ecosystem of the southern bay, Inhaca Island, Mozambique, *Hydrobiologia*, 428(1), 187–196.
- Bowen, A. J. (1969), The generation of longshore currents on a plane beach, *J. Mar. Res.*, 27, 206–215.
- Bowen, A. J., and D. L. Inman (1969), Rip currents: 2. Laboratory and field observations, *J. Geophys. Res.*, 74(23), 5479–5490.
- Burton, C., J. Izbicki, and K. Paybins (1998), Water quality trends in the Santa Ana River at MWD crossing and below Prado Dam, Riverside County, California, *U.S. Geol. Surv. Water Resour. Invest. Rep.*, 97-4173.
- CDIP (2003), Coastal Data Information Program, Scripps Inst. of Oceanogr., San Diego, Calif. (Available at [http://cdip.ucsd.edu/cdip\\_htmls/data.shtml](http://cdip.ucsd.edu/cdip_htmls/data.shtml))
- Cheng, N., A. W. Law, and A. N. Findikakis (2000), Oil transport in the surf zone, *J. Hydraul. Eng.*, 126(11), 803–809.
- Culliton, T. J. (1998), Population, distribution, density and growth; A state of the coast report, NOAA's state of the coast report; Natl. Oceanic and Atmos. Admin., Silver Spring, Md.
- Dwight, R. H., J. C. Semenza, D. B. Baker, and B. H. Olson (2002), Association of urban runoff with coastal water quality in Orange County, California, *Water Environ. Res.*, 74, 82–90.
- Dwight, R. H., D. B. Baker, J. C. Semenza, and B. H. Olson (2004), Health effects associated with recreational coastal water use: Urban vs rural California, *Am. J. Public Health*, 94(4), 565–567.
- Dwight, R. H., L. M. Fernandez, D. B. Baker, J. C. Semenza, and B. H. Olson (2005), Estimating the economic burden from illnesses associated with recreational coastal water pollution—A case study in Orange County, California, *J. Environ. Manage.*, in press.
- Elwany, M. H. S., R. E. Flick, and S. Ajaz (1998), Opening and closure of a marginal southern California lagoon inlet, *Estuaries*, 21(2), 246–254.
- Fischer, H. B., E. J. List, R. C. Y. Koh, J. Imberger, and N. H. Brooks (1979), *Mixing in Inland and Coastal Waters*, Elsevier, New York.
- Geldreich, E. E. (1976), Faecal coliform and faecal streptococcus density relationships in waste discharges and receiving waters, *Critical Rev. Environ. Contr.*, 6, 349–369.
- Grant, S. B., et al. (2000), Beach water quality investigation phase II: An analysis of ocean, surf zone, watershed, sediment and groundwater data collected from June 1998 through September 2000, City of Huntington Beach, Calif.
- Grant, S. B., et al. (2001), Generation of enterococci bacteria in a coastal saltwater marsh and its impact on surf zone water quality, *Environ. Sci. Technol.*, 35(12), 2407–2416.
- Grant, S. B., et al. (2002), Coastal runoff impact study phase III: Sources and dynamics of fecal indicators in the lower Santa Ana River watershed, Natl. Water Res. Inst., Burlington, Ont., Canada.
- Haile, R. W., et al. (1999), The health effects of swimming in ocean water contaminated by storm drain runoff, *Epidemiology*, 10(4), 355–363.
- Healy, M. G., and K. Hickey (2002), Historic land reclamation in the intertidal wetlands of the Shannon Estuary, western Ireland, *J. Coastal Res.*, 36, 365–373.
- Inman, D. L., and B. M. Brush (1973), Coastal challenge, *Science*, 181(4094), 20–32.
- Inman, D. L., R. J. Tait, and C. E. Nordstrom (1971), Mixing in surf zone, *J. Geophys. Res.*, 76(15), 3493–3514.
- Jeong, Y., et al. (2005), Identifying pollutant sources in tidally mixed systems: Case study of fecal indicator bacteria in Newport Bay, southern California, *Environ. Sci. Technol.*, in press.
- Jiang, S. C., and W. Chu (2004), PCR detection of pathogenic viruses in southern California urban rivers, *J. Appl. Microbiol.*, 97, 17–28.
- Jiang, S. C., R. Nobel, and W. Chu (2001), Human adenoviruses and coliphage in urban runoff-impacted coastal waters of southern California, *Appl. Environ. Microbiol.*, 67, 179–184.
- Jones, B. H., M. A. Noble, and T. D. Dickey (2002), Hydrographic and particle distributions over the Palos Verdes Continental Shelf: Spatial, seasonal and daily variability, *Cont. Shelf Res.*, 22, 945–965.
- Kim, J. H. (2004), Fecal pollution in coastal waters: Sources, transport, and public notification, Ph.D. thesis, Univ. of Calif., Irvine.
- Kim, J. H., and S. B. Grant (2004), Public mis-notification of coastal water quality: A probabilistic analysis of posting errors at Huntington Beach, California, *Environ. Sci. Technol.*, 38, 2626–2636.

- Kim, J. H., S. B. Grant, C. D. McGee, B. F. Sanders, and J. L. Largier (2004), Locating sources of surf zone pollution: A mass budget analysis of fecal indicator bacteria at Huntington Beach, California, *Environ. Sci. Technol.*, *38*, 2497–2505.
- Kirby, J. T. (1986), Higher-order approximation in the parabolic equation method for water waves, *J. Geophys. Res.*, *91*(C1), 933–952.
- Kjerfve, B., and K. E. Magill (1989), Geographic and hydrodynamic characteristics of shallow coastal lagoons, *Mar. Geol.*, *88*, 187–199.
- Koh, R. C. Y., and N. H. Brooks (1975), Fluid mechanics of wastewater disposal in the ocean, *Ann. Rev. Fluid Mech.*, *7*, 187–211.
- KOMEX H<sub>2</sub>O Science Incorporated (2003), AES Huntington Beach Generating Station Surf Zone Water Quality Study, Calif. Energy Comm., Sacramento.
- Longuet-Higgins, M. S. (1953), Mass transport in water waves, *Philos. Trans., Ser. A*, *245*, 535–581.
- Longuet-Higgins, M. S. (1970a), Longshore currents generated by obliquely incident sea waves 1, *J. Geophys. Res.*, *75*, 6778–6789.
- Longuet-Higgins, M. S. (1970b), Longshore currents generated by obliquely incident sea waves 2, *J. Geophys. Res.*, *75*, 6790–6801.
- Longuet-Higgins, M. S., and R. W. Stewart (1964), Radiation stresses in water waves; a physical discussion, with applications, *Deep Sea Res.*, *11*, 529–563.
- Murray, C. J., H. J. Lee, and M. A. Hampton (2002), Geostatistical mapping of effluent-affected sediment distribution on the Palos Verdes Shelf, *Cont. Shelf Res.*
- Noble, M., and J. Xu (2004), Coastal circulation and transport patterns: The likelihood of OCSD's plume impacting Huntington Beach shoreline, *U.S. Geol. Surv. Open File Rep.*, *2004-1019*.
- O'Reilly, W. C., and R. T. Guza (1991), Comparison of spectral refraction and refraction-diffraction wave models, *J. Waterw. Port Coastal Ocean Eng.*, *117*, 199–215.
- Pruss, A. (1998), Review of epidemiological studies on health effects from exposure to recreational water, *Int. J. Epidemiol.*, *27*(1), 1–9.
- Raubenheimer, B., and R. T. Guza (1996), Wave transformation across the inner surf zone, *J. Geophys. Res.*, *101*(C11), 25,575–25,597.
- Reeves, R. L., S. B. Grant, R. D. Mrse, C. M. Copil Oancea, B. F. Sanders, and A. B. Boehm (2004), Scaling and management of fecal indicator bacteria in runoff from a coastal urban watershed in southern California, *Environ. Sci. Technol.*, *38*, 2637–2648.
- Sanders, B. F., C. L. Green, A. L. Chu, and S. B. Grant (2001), Case study: Modeling tidal transport of urban runoff in channels using the finite-volume method, *J. Hydraul. Eng.*, *127*, 795–804.
- Schiff, K. C., M. J. Allen, E. Y. Zeng, and S. M. Bay (2000), Southern California, *Mar. Pollut. Bull.*, *41*(1–6), 76–93.
- Shuval, H. (2003), Estimating the global burden of thalassogenic diseases: Human infectious diseases caused by wastewater pollution of the marine environment, *J. Water Health*, *1*, 53–64.
- Sinton, L. W., R. K. Finlay, and P. A. Lynch (1999), Sunlight inactivation of fecal bacteriophages and bacteria in sewage-polluted seawater, *Appl. Environ. Microbiol.*, *65*(8), 3605–3613.
- Smart, P. L., and I. M. S. Laidlaw (1977), An evaluation of some fluorescent dyes for water tracing, *Water Resour. Res.*, *13*(1), 15–33.
- Snodgrass, F. E., G. W. Grove, K. F. Hasselma, G. R. Miller, W. H. Munk, and W. H. Powers (1966), Propagation of ocean swell across Pacific, *Philos. Trans. R. Soc. London, Ser. A*, *259*(1103), 505–584.
- Steets, B. M., and P. A. Holden (2003), A mechanistic model of runoff-associated fecal coliform fate and transport through a coastal lagoon, *Water Res.*, *37*, 589–608.
- Turbow, D. J., N. D. Osgood, and S. C. Jiang (2003), Evaluation of recreational health risk in coastal waters based on enterococcus densities and bathing patterns, *Environ. Health Perspect.*, *111*(4), 598–603.
- Warrick, J. A., L. A. K. Mertes, L. Washburn, and D. A. Siegel (2004), Dispersal forcing of southern California river plumes, based on field and remote sensing observations, *Geo Mar. Lett.*, *24*, 46–52.
- Washburn, L., K. A. McClure, B. H. Jones, and S. M. Bay (2003), Spatial scales and evolution of stormwater plumes in Santa Monica Bay, *Mar. Environ. Res.*, *56*, 103–125.

---

C. Cudaback, Marine Earth and Atmospheric Science, North Carolina State University, Campus Box 8208, Raleigh, NC 27695-8208, USA. (cncudaba@ncsu.edu)

S. B. Grant, Department of Chemical Engineering and Material Sciences, University of California, Irvine, CA 92697, USA. (sbgrant@uci.edu)

S. A. Jenkins and J. Wasyl, Scripps Institution of Oceanography, University of California, San Diego, CA 92093, USA. (sajenkins@ucsd.edu; jwasyl@ucsd.edu)

B. H. Jones, Department of Biological Sciences, University of Southern California, Los Angeles, CA 90089, USA. (bjones@usc.edu)

J. H. Kim, Department of Environmental Science and Engineering, Gwangju Institute of Science and Technology, 1 Oryong-dong, Buk-gu, Gwangju 500-712, Korea. (joonkim@gist.ac.kr.edu)